
A Linear Approach to Data Poisoning

D. G. M. Flynn
Mathematical Institute, Oxford

Diego Granziol
Mathematical Institute, Oxford

Abstract

Backdoor and data-poisoning attacks can flip predictions with tiny training corruptions, yet a sharp theory linking poisoning strength, overparameterization, and regularization is lacking. We analyze ridge least squares with an unpenalized intercept in the high-dimensional regime $p, n \rightarrow \infty$, $p/n \rightarrow c$. Targeted poisoning is modelled by shifting a θ -fraction of one class by a direction \mathbf{v} and relabelling. Using resolvent techniques and deterministic equivalents from random matrix theory, we derive closed-form limits for the poisoned score explicit in the model parameters. The formulas yield scaling laws, recover the interpolation threshold as $c \rightarrow 1$ in the ridgeless limit, and show that the weights align with the poisoning direction. Synthetic experiments match theory across sweeps of the parameters and MNIST backdoor tests show qualitatively consistent trends. The results provide a tractable framework for quantifying poisoning in linear models.

1 Introduction

Backdoor and data-poisoning attacks can subvert modern ML systems with small, targeted changes to the training data. Empirically, even tiny poisoned fractions imprint triggers that flip predictions at test time while leaving standard accuracy intact, across supervised and contrastive pretraining regimes (Gu et al., 2017; Turner et al., 2019; Shafahi et al., 2018; Carlini & Terzis, 2022; Xu et al., 2024). Despite extensive empirical evidence and many attack variants, sharp theory quantifying *how* poisoning strength, overparameterization, and regularization interact to control attack efficacy remains limited.

Recent research has extended the study of data poisoning and backdoor attacks into the domain of large language models (LLMs), demonstrating that vulnerabilities persist even at scale. Instruction-tuned LLMs can

be manipulated with only a small fraction of poisoned examples, leading to persistent triggers that reliably alter outputs without degrading overall utility (Zhou et al., 2025). Beyond classical poisoning, methods such as direct model editing enable attackers to implant backdoors efficiently into pretrained weights (Li et al., 2024). Benchmarks confirm that LLMs present multiple attack surfaces, including fine-tuning pipelines, prompt injection, and system-level instructions, making them especially susceptible to both prompt-based triggers (Yao et al., 2023) and stealthy manipulation of instruction hierarchies (Zhang et al., 2024b; Zhou et al., 2024). Recent analyses further indicate that poisoning in LLMs interacts with data contamination and emergent behavior in complex ways, highlighting that backdoor robustness must be considered a critical property of foundation models (He et al., 2025; Ge et al., 2024).

AI ethics and governance motivation. Backdoor and data-poisoning risks are recognized as first-class threats in modern AI governance. The EU AI Act explicitly lists data poisoning as a cyber-risk for “high-risk” systems, mandating robustness, transparency, and lifecycle security (EUA, a,b). The NIST AI Risk Management Framework and AML taxonomy similarly highlight poisoning as a cross-cutting vulnerability requiring measurable safeguards and incident response (Tabassi et al., 2023; of Standards & Technology, 2024; Vassilev et al., 2025). Operational frameworks such as MITRE ATLAS and OWASP’s Top-10 for LLM/GenAI catalog poisoning and backdoor tactics as key adversarial classes (MIT; OWA, b,a). Accountability artifacts—including Datasheets for Datasets, Model Cards, and AI FactSheets—stress provenance and risk documentation, for which solution-shift diagnostics (e.g., weight projections, curvature analysis) offer auditable evidence (Geburu et al., 2021; Mitchell et al., 2019; Arnold et al., 2019). Beyond compliance, malicious-use analyses underscore the societal stakes of covert model manipulation (Brundage et al., 2018), while sustainability perspectives emphasize efficient defenses that enable targeted remediation without full retraining (Schwartz et al., 2020). Together, these considerations

motivate principled methods that measure and explain how solutions move under poisoning, aligning technical robustness with governance and accountability.

AI theory motivation. Early work on general poisoning without backdoor triggers established worst-case guarantees for ERM with outlier-removal defences (Steinhardt et al., 2017) and showed, in the regression setting, how bi-level optimization attacks can shift learned solutions while trimmed estimators offer provable robustness (Jagielski et al., 2018). A distinct line of work exploits the structure of backdoors: poisoned examples form mixtures with shifted means, producing identifiable spectral signatures that align with the trigger direction (Tran et al., 2018), with later refinements using robust statistics to tolerate higher contamination (Hayase et al., 2021) and certified detectors that guarantee detectability when shifts exceed a threshold (Xiang et al., 2023). Others provide robustness certificates against triggers, for example through randomized smoothing (Wang et al., 2020) or federated learning schemes with clipping and smoothing (Xie et al., 2021), while mechanistic analyses formalize when backdoors are learnable, tying vulnerability to excess capacity (Manoj & Blum, 2021), orthogonality of gradients and decision regions (Zhang et al., 2024a), and adaptability directions in classical learners (Xian et al., 2023); at the extreme, cryptographic constructions show that undetectable backdoors exist in principle (Goldwasser et al., 2022). Whereas these works primarily establish detection criteria, certification bounds, or conditions for learnability, our contribution is complementary: we provide closed-form, high-dimensional limit laws for poisoned ridge least squares, giving explicit scaling in $(\theta, |\mathbf{v}|, \lambda, c)$ and showing estimator alignment with the trigger direction, thereby turning qualitative vulnerability into quantitative *solution deltas* that can serve as auditable, governance-ready measures of poisoning efficacy.

RMT theory motivation. Random matrix theory yields sharp asymptotics for ridge regression in the proportional high-dimensional regime. Classical results give deterministic equivalents for spectra and risk, leading to closed-form formulas for prediction error and optimal regularization (Dobriban & Wager, 2018; Hastie et al., 2019; Couillet & Liao, 2022b; Mei et al., 2019). These works position RMT as a lens on bias–variance trade-offs, double descent, and kernel generalization, but they have not been developed from a security or poisoning perspective. In particular, while spectral methods underpin many empirical defenses against backdoors, a full RMT framework for quantifying adversarial vulnerabilities or solution shifts under poisoning remains essentially absent.

2 Contributions and Results in brief

Our work develops a tractable random matrix framework for quantifying the impact of targeted backdoor poisoning on high-dimensional ridge least squares. The main findings and contributions are as follows.

Takeaway I: Bigger is Better

For the same amount of data, larger models are more robust to a fixed fraction of data poisoning.

Takeaway II: Regularisation does not help

The effect of regularisation is small, as the contributions from the mean and variance are in opposite directions.

Framework and scope. We analyze ridge least squares with an unpenalized intercept in the high-dimensional regime $p, n \rightarrow \infty$ with $p/n \rightarrow c \in (0, \infty)$. We assume a random data and labels model, in order to focus on the effect of adding the poisoning. The theoretical work assumes that labels are independent of the data, however we include MNIST experiments that go beyond this setting.

Poisoning is targeted and structured: a θ -fraction of one class is shifted by a direction \mathbf{v} and relabelled. This Gaussian, rank-one contamination model provides analytic clarity and yields testable predictions. Section 3 details the assumptions, Section 4 gives the analytic results, Section 5 outlines the proof strategy, and Section 6 reports synthetic and image-domain experiments.

Model motivation We wish to develop the simplest model that is able to capture the essence of data poisoning. We will then test the predictions from our model against real data to verify that we have captured true behaviour. To this end, we consider a signal free model, formed of Gaussian data \mathbf{x} , which is mapped to a randomly chosen label $y \in \{-1, +1\}$. We then perform the “poisoning”, by adding a spike (a vector \mathbf{v}) to our data \mathbf{x} and changing the label, a setting considered empirically for example in Gu et al. (2017) Section 4. In an image setting this corresponds to 1.

Our empirical claim is that the shift caused in the high dimensional regressor from this spike is largely independent of the underlying data distribution, and so whether this is a signal free Gaussian, or the highly non-Gaussian anisotropic MNIST dataset, we see similar behaviour Figure (4). By studying in depth the former, we are then able to match trends and get insight into the latter.

We note additionally that we model the poisoning direction to be fixed rather than trained. We take some fixed \mathbf{v} and examine the behaviour based on this (and indeed we see that this depends only on $\|\mathbf{v}\|$ in our model). This is a distinct phenomenon to that of adversarial attacks, which has received large amounts of attention in the literature beginning with [Szegedy et al. \(2014\)](#). In an adversarial attack, the model is taken as given and the dataset is assumed to be “clean”, and the attack is to find a small perturbation of the input that results in a shift in the prediction.

Closed-form limit law. We prove that the poisoned predictor admits an asymptotic Gaussian distribution,

$$\hat{\beta}^\top(\mathbf{x}_0 + \mathbf{v}) \xrightarrow{d} \mathcal{N}(\mu, \sigma^2),$$

with explicit expressions for the mean shift $\mu(\theta, \|\mathbf{v}\|, \lambda, c)$ and variance $\sigma^2(\theta, \|\mathbf{v}\|, \lambda, c)$. These formulas yield a direct efficacy proxy

$$\eta = 1 - \Phi(-\mu/\sigma)$$

for backdoor success, where Φ is the CDF of $\mathcal{N}(0, 1)$.

Alignment with the trigger. The estimator $\hat{\beta}$ concentrates onto the poisoning direction \mathbf{v} : the alignment coefficient grows with the poisoning rate θ and diminishes with stronger regularization λ , making explicit how ridge penalization counteracts trigger imprinting.

Scaling laws and interpolation effects. The theory isolates the separate roles of poisoning fraction, trigger norm, regularization, and aspect ratio. In particular, in the ridgeless limit the variance term reproduces the interpolation threshold blow-up as $c \rightarrow 1$, and we also see for small θ that the poison efficacy has a linear effect in θ .

Validation. Synthetic experiments confirm the closed-form predictions across wide sweeps of $(c, \lambda, \|\mathbf{v}\|, \theta)$, while MNIST backdoor experiments reproduce the predicted scaling trends for the mean shift μ and show qualitatively consistent though noisier variance behaviour. These findings support the use of the linear RMT theory as a heuristic lens for understanding poisoning in more complex models.

3 Model and assumptions

We take a clean dataset, with isotropic Gaussian vectors, and we assume the labels are unstructured. Since we are including the centring in our model (via the bias) to remove the mean, this assumption amounts to discounting the covariance structure of our dataset.

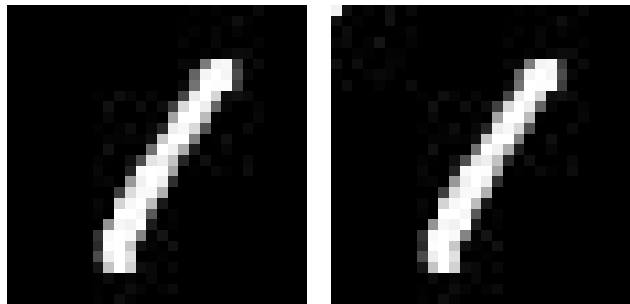
Assumption 3.1 (Clean data). Let $\mathbf{X} = [\mathbf{x}_1, \dots, \mathbf{x}_n] \in \mathbb{R}^{p \times n}$ be the data matrix and

$\mathbf{y} = (y_1, \dots, y_n) \in \{-1, +1\}^n$ the labels. Assume

$$\mathbb{P}(y_i = 1) = \mathbb{P}(y_i = -1) = \frac{1}{2} \quad \text{independently over } i,$$

and that $\mathbf{x}_i \sim \mathcal{N}(0, \mathbf{I}_p)$. All samples (\mathbf{x}_i, y_i) are independent across i .

We analyse the case where the poisoning amounts to adding a small feature perturbation to elements of one class, while changing the label to the other class in a binary setting. This follows the backdoor poisoning setup originally proposed in [Gu et al. \(2017\)](#).



(a) Unpoisoned

(b) Poisoned

Figure 1: An example of the poisoning mechanism, a small perturbation is made in the top left of the image. The left image is correctly labelled as "1", and the right image has its label changed to "0" in the poisoned dataset.

Assumption 3.2 (Poisoning mechanism). Fix $\theta \in [0, 1]$ and a direction $\mathbf{v} \in \mathbb{R}^p$ with $\|\mathbf{v}\| = O(1)$. Define an indicator vector $\mathbf{u} \in \{0, 1\}^n$ with

$$\mathbb{P}(u_i = 1 | y_i) = \begin{cases} \theta, & y_i = -1, \\ 0, & y_i = +1, \end{cases} \quad \text{independently over } i.$$

For $u_i = 1$ the attacker shifts the feature by \mathbf{v} and flips its label to $+1$; otherwise the sample is unchanged. Equivalently,

$$\mathbf{x}_i^{\text{pois}} = \mathbf{x}_i + \mathbf{v} u_i, \quad y_i^{\text{pois}} = y_i + 2u_i,$$

or, in matrix form,

$$\mathbf{X}^{\text{pois}} = \mathbf{X} + \mathbf{v} \mathbf{u}^\top, \quad \mathbf{y}^{\text{pois}} = \mathbf{y} + 2\mathbf{u}.$$

Conditionally, this yields

$$\mathbf{x}_i^{\text{pois}} \sim \begin{cases} \mathcal{N}(0, \mathbf{I}_p), & u_i = 0. \\ \mathcal{N}(\mathbf{v}, \mathbf{I}_p), & u_i = 1. \end{cases}$$

Finally, we assume that we are in a high-dimensional regime, where p the dimension of our data and n the number of data points are comparable and large. This regime is common in random matrix analysis of machine

learning, and is able to much more accurately capture behaviour than the classical limit where we fix p and take $n \rightarrow \infty$ Couillet & Liao (2022a); Vershynin (2018); Wainwright (2019). We take $p, n \rightarrow \infty$ in our analytic results, and we verify the results experimentally for large fixed p, n .

Assumption 3.3 (High-dimensional regime). We let $n, p \rightarrow \infty$ with $p/n \rightarrow c \in (0, \infty)$. All parameters (θ, λ, c) are fixed as $n, p \rightarrow \infty$ and we assume that $\|\mathbf{v}\| = O(1)$.

Model. We use ridge least squares with an *unpenalized* intercept b_0 :

$$\mathcal{L}(\boldsymbol{\beta}, b_0) = \frac{1}{n} \sum_{i=1}^n (\boldsymbol{\beta}^\top \mathbf{x}_i^{\text{pois}} + b_0 - y_i^{\text{pois}})^2 + \lambda \|\boldsymbol{\beta}\|^2 \quad (1)$$

$$(\hat{\boldsymbol{\beta}}, \hat{b}_0) = \arg \min_{(\boldsymbol{\beta}, b_0) \in \mathbb{R}^p \times \mathbb{R}} \mathcal{L}(\boldsymbol{\beta}, b_0; \mathbf{X}^{\text{pois}}, \mathbf{y}^{\text{pois}}, \lambda) \quad (2)$$

Let $\bar{\mathbf{x}} = \mathbb{E}[\frac{1}{n} \mathbf{X}^{\text{pois}} \mathbf{1}]$, $\bar{w} = \mathbb{E}[\frac{1}{n} \mathbf{1}^\top \mathbf{y}^{\text{pois}}]$, and define centred variables $\tilde{\mathbf{X}} = \mathbf{X}^{\text{pois}} - \bar{\mathbf{x}} \mathbf{1}^\top$, $\tilde{\mathbf{w}} = \mathbf{y}^{\text{pois}} - \bar{w} \mathbf{1}$. The estimator equals

$$\hat{\boldsymbol{\beta}} = \frac{1}{n} \left(\frac{1}{n} \tilde{\mathbf{X}} \tilde{\mathbf{X}}^\top + \lambda \mathbf{I}_p \right)^{-1} \tilde{\mathbf{X}} \tilde{\mathbf{w}}, \quad \hat{b}_0 = \bar{w} - \hat{\boldsymbol{\beta}}^\top \bar{\mathbf{x}}. \quad (3)$$

In particular, under assumptions 3.1 and 3.2 we have $\bar{\mathbf{x}} = \frac{\theta}{2} \mathbf{v}$, $\bar{w} = \theta$, and with $\mathbf{r} := \mathbf{u} - \frac{\theta}{2} \mathbf{1}$, $\tilde{\mathbf{X}} = \mathbf{X} + \mathbf{v} \mathbf{r}^\top$, $\tilde{\mathbf{w}} = \mathbf{y} + 2\mathbf{r}$.

4 Main result

We evaluate the behaviour of the poisoned model on a new independent poisoned test sample $\mathbf{x}_0 + \mathbf{v}$, where $\mathbf{x}_0 \sim \mathcal{N}(0, \mathbf{I}_p)$ is independent of the training set.

Theorem 4.1 (Asymptotic distribution under poisoning). *Under assumptions 3.1-3.3, as $n, p \rightarrow \infty$ with $p/n \rightarrow c \in (0, \infty)$, the scalar output of the poisoned regressor satisfies*

$$\hat{\boldsymbol{\beta}}^\top (\mathbf{x}_0 + \mathbf{v}) \xrightarrow{D} \mathcal{N}(\mu, \sigma^2), \quad (4)$$

where

$$\mu = \frac{\theta(1-\theta)m(-\lambda)\|\mathbf{v}\|^2}{(1+cm(-\lambda))(2+\|\mathbf{v}\|^2\theta(1-\frac{\theta}{2})(1-\lambda m(-\lambda)))}, \quad (5)$$

$$\sigma^2 = \left(\tilde{m}(-\lambda) - \lambda \tilde{m}'(-\lambda) \right) \left[(1-\theta^2) + \left(\frac{1+c^{-1}\tau^2}{(1+c^{-1}\tau^2(1-\lambda\tilde{m}(-\lambda)))^2} - 1 \right) \frac{\theta(1-\theta)^2}{2-\theta} \right], \quad (6)$$

with $\tau^2 = \|\mathbf{v}\|^2 \frac{\theta}{2} (1 - \frac{\theta}{2})$.

and $m(z)$ is the Stieltjes transform of the Marčenko–Pastur distribution with parameter c , given by

$$m(z) = \frac{1-c-z - \sqrt{(1-c-z)^2 - 4cz}}{2cz}, \quad (7)$$

and

$$\tilde{m}(z) = cm(z) - \frac{1-c}{z}. \quad (8)$$

Remark 4.2 (Limit for vanishing regularization). When $\lambda \rightarrow 0$ and $c < 1$, (5)–(6) reduce to

$$\mu_0 = \frac{\|\mathbf{v}\|^2 \theta (1-\theta)}{2 + \|\mathbf{v}\|^2 \theta (1 - \frac{\theta}{2})}, \quad (9)$$

$$\sigma_0^2 = \frac{c}{1-c} \left[(1-\theta^2) + \left(\frac{1+c^{-1}\tau^2}{(1+\tau^2)^2} - 1 \right) \frac{\theta(1-\theta)^2}{2-\theta} \right]. \quad (10)$$

Remark 4.3 (Poisoning efficacy). For a binary classifier with decision threshold 0, the poisoning efficacy is

$$\eta_{\text{pois}} = 1 - \Phi\left(-\frac{\mu}{\sigma}\right), \quad (11)$$

where Φ is the CDF of $\mathcal{N}(0, 1)$. For small θ , the model predicts $\eta_{\text{pois}} \approx 0.5 + O(\theta)$, consistent with empirical observations.

Proposition 4.4 (Alignment with poisoning vector). *Under assumptions 3.1-3.3 the estimator $\hat{\boldsymbol{\beta}}$ aligns asymptotically with \mathbf{v} :*

$$\hat{\boldsymbol{\beta}}^\top \mathbf{a} \xrightarrow{a.s.} C \mathbf{v}^\top \mathbf{a}, \quad C = \frac{\theta(1-\theta)m(-\lambda)}{(1+cm(-\lambda))(2+\|\mathbf{v}\|^2\theta(1-\frac{\theta}{2})(1-\lambda m(-\lambda)))}, \quad (12)$$

for any deterministic $\mathbf{a} \in \mathbb{R}^p$. Thus C increases with θ and decreases with λ .

5 Proof sketch

We outline the argument leading to the Gaussian limit and the closed forms for μ and σ^2 . Full proofs, including concentration and leave-one-out estimates, are deferred to the Appendix.

Methods The overarching idea is to use the Woodbury Lemma, an algebraic matrix identity:

Lemma 5.1 (Woodbury Formula (circa 1950)). *For $\mathbf{A} \in \mathbb{R}^{p \times p}$, $\mathbf{U}, \mathbf{V} \in \mathbb{R}^{p \times d}$, such that both \mathbf{A} and $\mathbf{A} + \mathbf{U}\mathbf{V}^\top$ are invertible, we have*

$$(\mathbf{A} + \mathbf{U}\mathbf{V}^\top)^{-1} = \mathbf{A}^{-1} - \mathbf{A}^{-1} \mathbf{U} (\mathbf{I}_d + \mathbf{V}^\top \mathbf{A}^{-1} \mathbf{U})^{-1} \mathbf{V}^\top \mathbf{A}^{-1}$$

Crucially here, if p is large and k is finite (in our case we use this for $k = 3$), then the inner matrix here

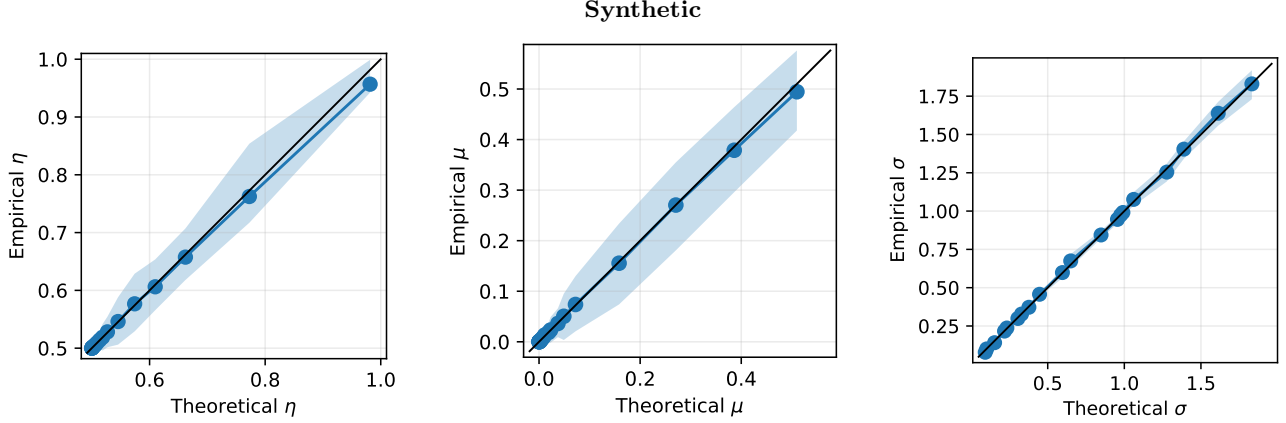


Figure 2: We plot empirical vs theoretical values for the derived η , μ and σ under the synthetic data model. We perform a parameter sweep across c , λ , $\|\mathbf{v}\|$ and θ , plotting the theoretical parameter against the empirical for each case. The circular marks are the averages over 100 independent trials, and the shaded region is the interquartile range.

is a small $k \times k$ inverse, and hence we do not have any issues interchanging matrix inversion and limits. This is fundamentally what allows us to control the behaviour of random matrices when they have a low-rank perturbation. This is used together with the fact that the unpoisoned Gaussian (Wishart) matrix has a well understood resolvent.

Specifically, we have that if $\mathbf{X} = [\mathbf{x}_1, \dots, \mathbf{x}_n] \in \mathbb{R}^{p \times n}$ is an isotropic Gaussian matrix, in the sense that $\mathbf{x}_i \sim \mathcal{N}(0, \mathbf{I}_p)$. Then defining

$$\mathbf{Q}_0(z) := \left(\frac{1}{n} \mathbf{X} \mathbf{X}^\top - z \mathbf{I}_p \right)^{-1},$$

we have that

$$\mathbf{Q}_0(z) \longleftrightarrow m(z) \mathbf{I}_p.$$

By " \longleftrightarrow " we mean becomes deterministically equivalent to - a notion we make precise in the appendix, where here $m(z)$ is the Stieltjes transform of the Marčenko-Pastur distribution - the connection to Stieltjes transforms comes in here as $\text{tr} \mathbf{Q}_0$ is the Stieltjes transform of the empirical distribution of the eigenvalues of \mathbf{X} . Informally however, this tells us that when we are taking linear functionals of the matrix \mathbf{Q}_0 , then we can simply replace it with $m(z) \mathbf{I}_p$.

Step 1: Centering and linearization. Recall the ridge estimator with unpenalized intercept from (3):

$$\begin{aligned} \hat{\boldsymbol{\beta}} &= \frac{1}{n} \left(\frac{1}{n} \tilde{\mathbf{X}} \tilde{\mathbf{X}}^\top + \lambda \mathbf{I}_p \right)^{-1} \tilde{\mathbf{X}} \tilde{\mathbf{w}}, \\ \hat{b}_0 &= \bar{w} - \hat{\boldsymbol{\beta}}^\top \bar{\mathbf{x}}. \end{aligned}$$

With $\mathbf{r} = \mathbf{u} - \frac{\theta}{2} \mathbf{1}$ we have

$$\begin{aligned} \tilde{\mathbf{X}} &= \mathbf{X} + \mathbf{v} \mathbf{r}^\top, \\ \tilde{\mathbf{w}} &= \mathbf{y} + 2\mathbf{r}, \end{aligned}$$

and the LLNs

$$\begin{aligned} \frac{1}{n} \|\mathbf{r}\|^2 &\xrightarrow{a.s.} s := \frac{\theta}{2} \left(1 - \frac{\theta}{2} \right), \\ \frac{1}{n} \mathbf{y}^\top \mathbf{r} &\xrightarrow{a.s.} -\frac{\theta}{2}, \\ \frac{1}{n} \mathbf{r}^\top \tilde{\mathbf{w}} &\xrightarrow{a.s.} \frac{\theta(1-\theta)}{2}. \end{aligned}$$

Let $z = -\lambda$, $\mathbf{Q}_1(z) = \left(\frac{1}{n} \tilde{\mathbf{X}} \tilde{\mathbf{X}}^\top - z \mathbf{I}_p \right)^{-1}$ and $\tilde{\mathbf{Q}}_1(z) = \left(\frac{1}{n} \tilde{\mathbf{X}}^\top \tilde{\mathbf{X}} - z \mathbf{I}_n \right)^{-1}$. Then

$$\hat{\boldsymbol{\beta}} = \frac{1}{n} \mathbf{Q}_1(-\lambda) \tilde{\mathbf{X}} \tilde{\mathbf{w}}.$$

Step 2: Rank-one spike and resolvent deterministic equivalents. Write the spike direction $\mathbf{a} := \mathbf{v} / \|\mathbf{v}\|$ and set

$$\tau^2 := \|\mathbf{v}\|^2 s = \|\mathbf{v}\|^2 \frac{\theta}{2} \left(1 - \frac{\theta}{2} \right).$$

The perturbation $\tilde{\mathbf{X}} = \mathbf{X} + \mathbf{v} \mathbf{r}^\top$ is rank one on each side of \mathbf{X} .

By the Woodbury Lemma, and the Deterministic equivalent of the Wishart Matrix, the resolvents admit deterministic equivalents that depend only on $m(z)$, $\tilde{m}(z)$, and τ^2 (see Appendix Lemmas A.1-A.2 following Couillet & Liao (2022a)):

$$\mathbf{Q}_1(z) \iff \tilde{\mathbf{Q}}_1(z)$$

$$\tilde{\mathbf{Q}}_1(z) = m(z) \left(\mathbf{I}_p - \frac{\tau^2 (1 + z m(z))}{1 + \tau^2 (1 + z m(z))} \mathbf{a} \mathbf{a}^\top \right),$$

$$\tilde{\mathbf{Q}}_1(z) \iff \tilde{m}(z) \left(\mathbf{I}_n - \frac{c^{-1} \tau^2 (1 + z \tilde{m}(z))}{1 + c^{-1} \tau^2 (1 + z \tilde{m}(z))} \bar{\mathbf{b}} \bar{\mathbf{b}}^\top \right),$$

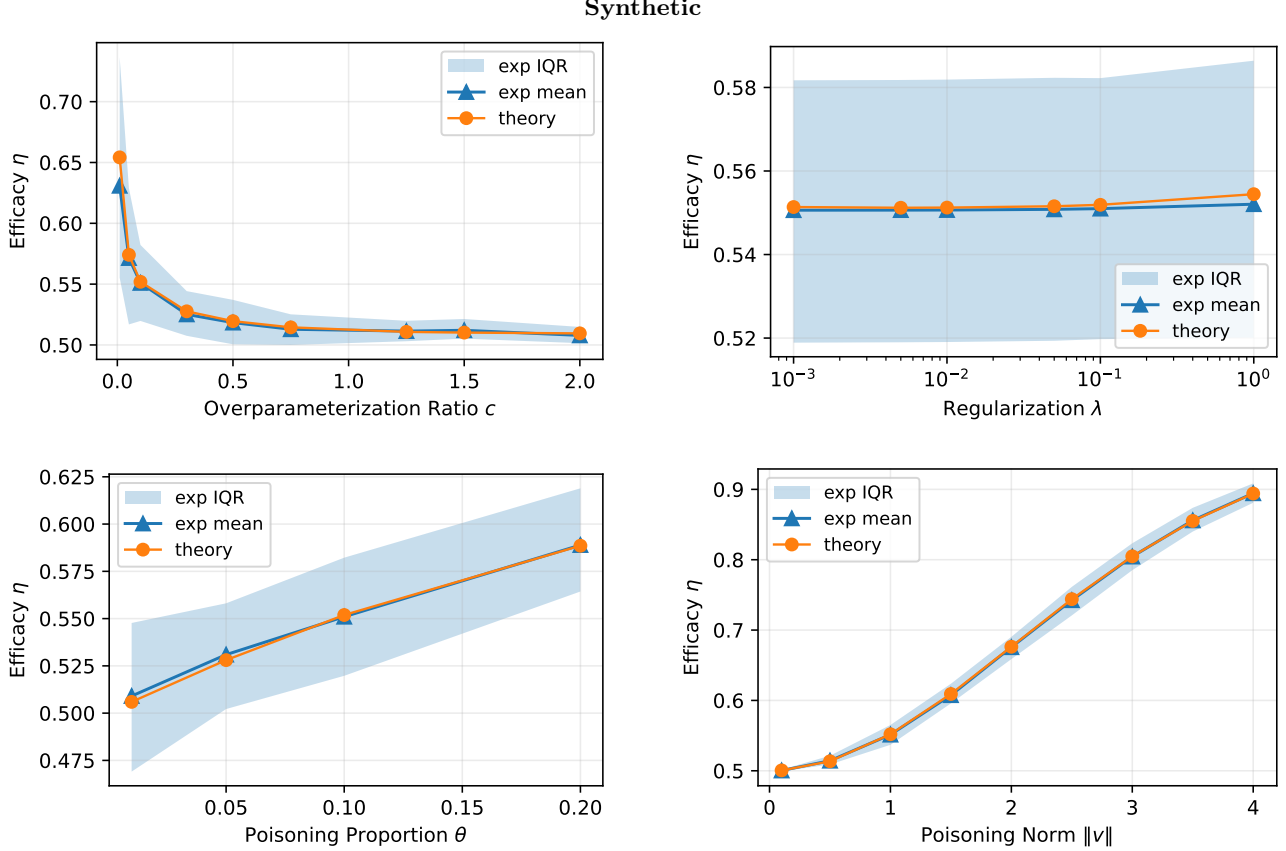


Figure 3: Plot of the poisoning efficacy η for the binary classifier on synthetic data, as the parameters vary. We use the fixed values $c = 0.1$, $\lambda = 0.1$, $\|v\| = 1$ and $\theta = 0.1$, and then vary each parameter in turn. The circles are the theoretical results, and the triangles are the experimental results, with the interquartile range shaded.

where $\bar{\mathbf{b}} := \mathbf{r}/\|\mathbf{r}\|$. For the squared resolvent one has

$$\begin{aligned} \tilde{\mathbf{Q}}_1(z)^2 &\iff \tilde{m}'(z)\mathbf{I}_n + \left(T(z) - \tilde{m}'(z)\right)\bar{\mathbf{b}}\bar{\mathbf{b}}^\top, \\ T(z) &= \frac{(c^{-1}\tau^2 + 1)\tilde{m}'(z) - c^{-1}\tau^2\tilde{m}(z)^2}{(1 + c^{-1}\tau^2(1 + z\tilde{m}(z)))^2}. \end{aligned}$$

Step 3: Mean of the poisoned score. We study the scalar $\hat{\beta}^\top \mathbf{v}$. Expanding $\tilde{\mathbf{X}} = \mathbf{X} + \mathbf{v}\mathbf{r}^\top$,

$$\begin{aligned} \hat{\beta} &= \frac{1}{n}\mathbf{Q}_1(-\lambda)(\mathbf{X}\mathbf{y} + 2\mathbf{X}\mathbf{r} \\ &\quad + \mathbf{v}\mathbf{r}^\top\mathbf{y} + 2\mathbf{v}\mathbf{r}^\top\mathbf{r}). \end{aligned}$$

By independence and centering, $\mathbb{E}[\mathbf{X}\mathbf{y}] = \mathbb{E}[\mathbf{X}\mathbf{r}] = \mathbf{0}$, so the contribution comes from the \mathbf{v} -term. A standard leave-one-out argument (Sherman–Morrison on \mathbf{Q}_1) yields the decoupling

$$\begin{aligned} \frac{1}{n}\mathbf{Q}_1(-\lambda)\mathbf{v}\mathbf{r}^\top\tilde{\mathbf{w}} &= \frac{1}{1 + cm(-\lambda)}\bar{\mathbf{Q}}_1(-\lambda)\mathbf{v} \cdot \frac{1}{n}\mathbf{r}^\top\tilde{\mathbf{w}} \\ &\quad + o_{\|\cdot\|}(1), \end{aligned}$$

where m is the Marcenko–Pastur Stieltjes transform. Using $\frac{1}{n}\mathbf{r}^\top\tilde{\mathbf{w}} \xrightarrow{a.s.} \frac{\theta(1-\theta)}{2}$ and $\bar{\mathbf{Q}}_1(-\lambda)\mathbf{v} = m(-\lambda)\mathbf{v}/(1 +$

$\tau^2(1 - \lambda m(-\lambda)))$, we obtain

$$\mathbb{E}[\hat{\beta}^\top \mathbf{v}] = \frac{m(-\lambda)}{1 + cm(-\lambda)} \cdot \frac{\frac{1}{2}\|\mathbf{v}\|^2\theta(1-\theta)}{1 + \tau^2(1 - \lambda m(-\lambda))} + o(1).$$

Rewriting $1 + \tau^2(1 - \lambda m) = \frac{1}{2}(2 + \|\mathbf{v}\|^2\theta(1 - \frac{\theta}{2}))(1 - \lambda m)$ gives the announced

$$\mu = \frac{\theta(1-\theta)m(-\lambda)\|\mathbf{v}\|^2}{(1 + cm(-\lambda))(2 + \|\mathbf{v}\|^2\theta(1 - \frac{\theta}{2}))(1 - \lambda m(-\lambda))}.$$

A Gaussian concentration (e.g. quadratic-forms close-to-trace and a Burkholder inequality) shows $\hat{\beta}^\top \mathbf{v} - \mathbb{E}[\hat{\beta}^\top \mathbf{v}] \rightarrow 0$; see Appendix.

Step 4: Variance via $\|\hat{\beta}\|^2$. For a fresh test point $\mathbf{x}_0 \sim \mathcal{N}(0, \mathbf{I}_p)$ independent of the training set, the only asymptotic randomness in $\hat{\beta}^\top(\mathbf{x}_0 + \mathbf{v})$ comes from \mathbf{x}_0 because $\hat{\beta}$ concentrates. Conditionally on $\hat{\beta}$, $\hat{\beta}^\top \mathbf{x}_0 \sim \mathcal{N}(0, \|\hat{\beta}\|^2)$, hence the asymptotic variance is $\sigma^2 = \lim \|\hat{\beta}\|^2$.

Using the identity

$$\frac{1}{n}\tilde{\mathbf{X}}^\top\mathbf{Q}_1(z)^2\tilde{\mathbf{X}} = z\tilde{\mathbf{Q}}_1(z)^2 + \tilde{\mathbf{Q}}_1(z),$$

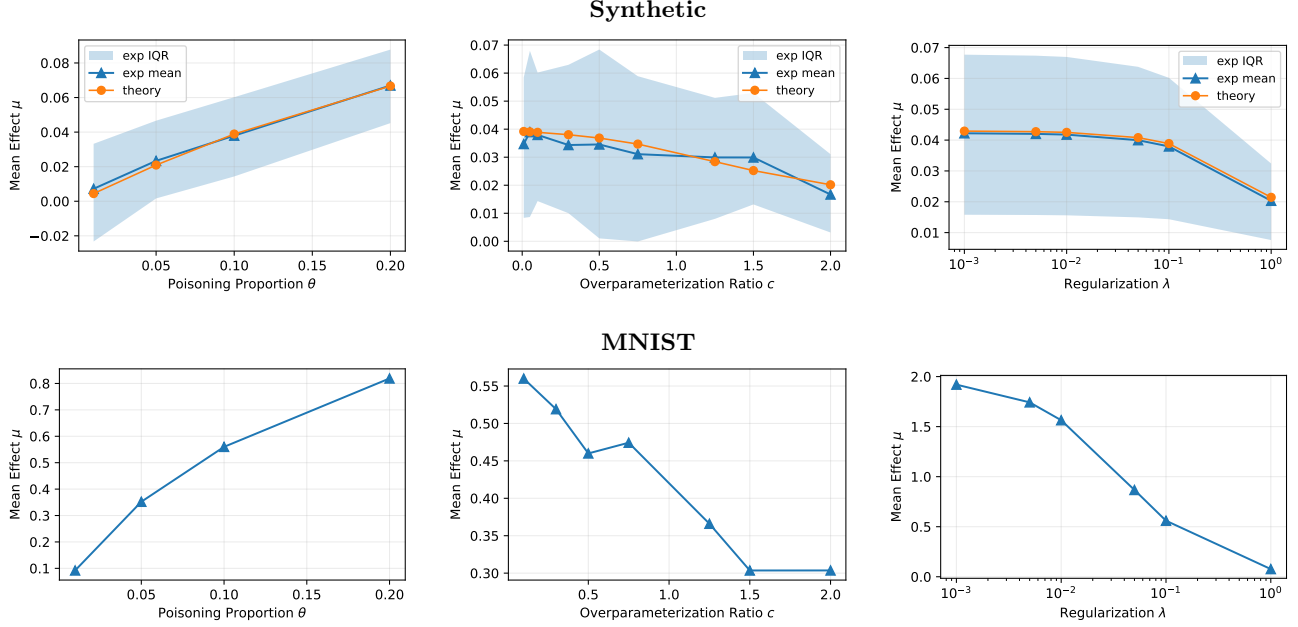


Figure 4: Top: empirical and theoretical results for the μ in the synthetic data model. We fix the values $c = 0.1$, $\|\mathbf{v}\| = 1$, $\theta = 0.1$, $\lambda = 0.1$, and then vary c , θ and λ . We fix $p = 500$ and vary n to get the required values of c . We plot the experimental mean and IQR across 100 independent samples. Bottom: We perform the poisoning and classification on MNIST. We use the same values of c , $\|\mathbf{v}\|$, θ and λ , and vary the number of data points included to control c . We do a binary classification on the digits "0" and "1".

we obtain

$$\|\hat{\beta}\|^2 = \frac{1}{n} \tilde{\mathbf{w}}^\top (z \tilde{\mathbf{Q}}_1(z)^2 + \tilde{\mathbf{Q}}_1(z)) \tilde{\mathbf{w}} \Big|_{z=-\lambda}.$$

Insert the Deterministic Equivalent from Step 2 and the LLNs

$$\begin{aligned} \frac{1}{n} \|\tilde{\mathbf{w}}\|^2 &\xrightarrow{a.s.} 1 - \theta^2, \\ \frac{1}{n} (\tilde{\mathbf{w}}^\top \bar{\mathbf{b}})^2 &\xrightarrow{a.s.} \frac{\theta(1-\theta)^2}{2-\theta}. \end{aligned}$$

Let $B(z) = 1 + c^{-1}\tau^2(1 + z\tilde{m}(z))$ and $S(z) = \tilde{m}(z) + z\tilde{m}'(z)$. A short algebraic manipulation (Appendix) shows

$$\begin{aligned} z(T(z) - \tilde{m}'(z)) - \tilde{m}(z) \left(1 - \frac{1}{B(z)}\right) \\ = S(z) \left(\frac{c^{-1}\tau^2 + 1}{B(z)^2} - 1\right). \end{aligned}$$

Therefore,

$$\begin{aligned} \|\hat{\beta}\|^2 &\rightarrow S(-\lambda) \left[(1 - \theta^2) \right. \\ &\left. + \left(\frac{1 + c^{-1}\tau^2}{(1 + c^{-1}\tau^2(1 - \lambda\tilde{m}(-\lambda)))^2} - 1 \right) \frac{\theta(1-\theta)^2}{2-\theta} \right], \end{aligned}$$

which is exactly (6) since $S(-\lambda) = \tilde{m}(-\lambda) - \lambda\tilde{m}'(-\lambda)$.

Step 5: Gaussian limit for the poisoned score.

Conditionally on the training set, $\hat{\beta}^\top \mathbf{x}_0 \sim \mathcal{N}(0, \|\hat{\beta}\|^2)$ and $\hat{\beta}^\top \mathbf{v} \rightarrow \mu$. Since $\|\hat{\beta}\|^2 \rightarrow \sigma^2$ in probability and \mathbf{x}_0 is independent, we get

$$\hat{\beta}^\top (\mathbf{x}_0 + \mathbf{v}) \xrightarrow{d} \mathcal{N}(\mu, \sigma^2).$$

Step 6: Alignment.

For any deterministic $\mathbf{a} \in \mathbb{R}^p$,

$$\mathbb{E}[\hat{\beta}^\top \mathbf{a}] = \frac{\frac{1}{2}\theta(1-\theta)}{1 + cm(-\lambda)} \mathbf{a}^\top \bar{\mathbf{Q}}_1(-\lambda) \mathbf{v} + o(1) \rightarrow C \mathbf{v}^\top \mathbf{a},$$

with

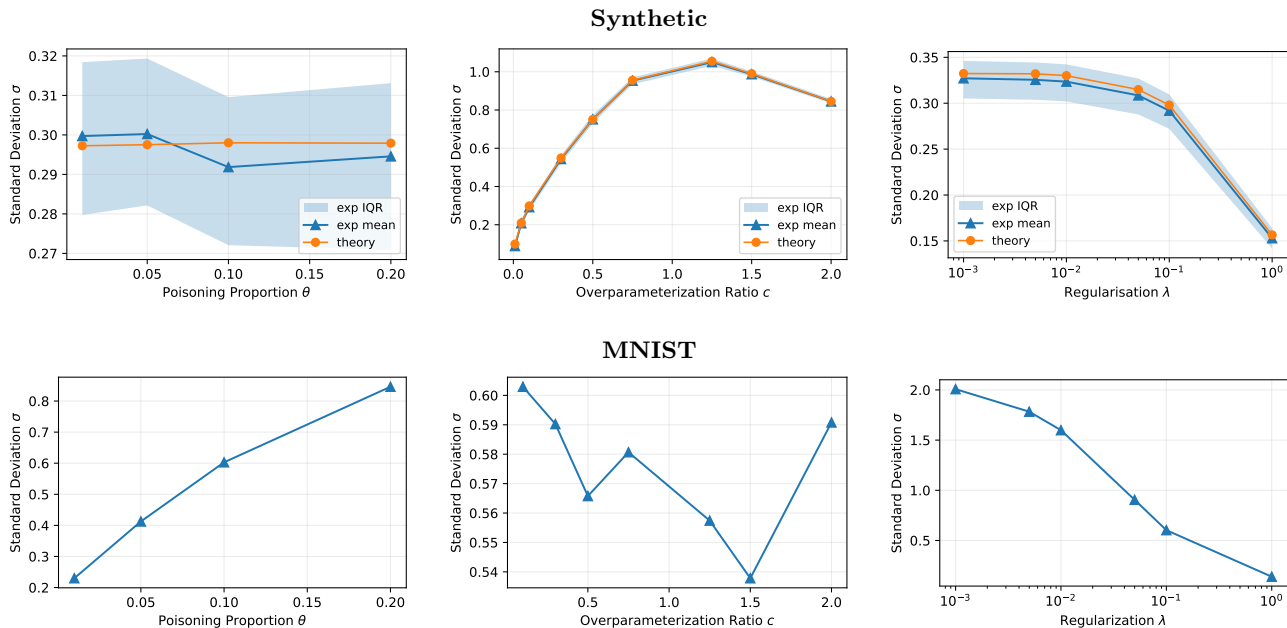
$$C = \frac{\theta(1-\theta)m(-\lambda)}{(1 + cm(-\lambda))(2 + \|\mathbf{v}\|^2\theta(1 - \frac{\theta}{2})(1 - \lambda m(-\lambda)))}.$$

Thus $\hat{\beta}$ asymptotically lies in the span of \mathbf{v} and the alignment increases with θ and decreases with λ .

Step 7: Checks and limits.

(i) No poisoning ($\theta = 0$) gives $\mu = 0$ and $\sigma^2 = \tilde{m}(-\lambda) - \lambda\tilde{m}'(-\lambda)$ (clean ridge). (ii) As $\lambda \rightarrow 0$ with $c < 1$, use $\tilde{m}(-\lambda) - \lambda\tilde{m}'(-\lambda) \rightarrow \frac{c}{1-c}$ and $1 - \lambda\tilde{m}'(-\lambda) \rightarrow c$ to recover the unregularized limits reported in the remarks. (iii) For small θ , $\mu/\sigma = O(\theta)$, matching the linear growth of attack efficacy.

Throughout we repeatedly use (a) Woodbury/Sherman–Morrison to isolate single-sample and spike effects;

Figure 5: Comparison for σ . The setup of the experiments is the same as in Figure 4.

(b) deterministic equivalents for spiked resolvents; (c) quadratic-form close-to-trace lemmas and Gaussian concentration to replace random denominators by their limits; and (d) leave-one-out resolvents to decouple dependencies between $\tilde{\mathbf{z}}_i$ and \mathbf{Q}_1 . Precise statements and bounds are in the Appendix, following the methodology of Couillet & Liao (2022a).

6 Discussion and Experiments

We perform experiments on the MNIST dataset Deng (2012), as well as the synthetic dataset generated procedurally by the setup of Assumptions 3.1, 3.2: we generate a Gaussian matrix with assigned labels and then apply the poisoning to a proportion θ of the data. We use a new random seed over each retry to produce the interquartile range shown on the figures. For both the synthetic and MNIST datasets, we perform the experiments using the explicit Equation 3, computing the matrix computations on an Nvidia 3080Ti GPU. We perform a parameter sweep over a range of $(\lambda, c, \|\mathbf{v}\|, \theta)$.

Parameter	Sweep Values
c	0.1, 0.3, 0.5, 0.75, 1.25, 1.5, 2.0
λ	0.001, 0.005, 0.01, 0.05, 0.1, 1.0
θ	0.01, 0.05, 0.1, 0.2
$\ \mathbf{v}\ $	0.1, 0.5, 1, 1.5, 2, 2.5, 3, 3.5, 4

Table 1: Parameter grid used for the sweep.

We choose the \mathbf{v} direction as shown in Figure 1. We fix

the dimension $p = 500$ for each synthetic plot, and vary the dataset size n accordingly to get required values of c . Similarly we vary n for the MNIST case to get the values of $c = 784/n$. We then compute μ via $\hat{\beta}^\top \mathbf{v}$ and σ^2 as $\hat{\beta}^\top \hat{\beta}$. We restrict to the binary case on MNIST, to the digits 0 and 1, labelled with $\{-1, +1\}$.

On the synthetic dataset, we find a strong verification of the theory, as shown in Figures 2 and 3. On each plot of the synthetic data we plot the empirically observed values in blue against the theoretical values from (5)–(6) in orange. Increasing poison rate θ and trigger strength $\|\mathbf{v}\|$ increases the mean shift μ and also increases the variance σ via τ^2 , yielding higher attack success $\eta = 1 - \Phi(-\mu/\sigma)$. In the synthetic dataset we see stronger regularization λ reduces μ and σ (with a stronger effect on σ) resulting in an increase of η with λ . Larger aspect ratio $c = p/n$ decreases μ and has a more varying effect on σ resulting in a general decrease in η as c increases.

On the MNIST dataset, we find good qualitative agreement between the theory and the practice on the mean (first-order effect) of the poisoning μ (Fig. 4). We see that the mean increases as θ increases, decreases with λ and decreases as c increases. In particular this means on a larger dataset of the same dimension, hence with $c = p/n$ smaller, then the average effect of poisoning is larger, *even while keeping the proportion the same*.

For the second order effect σ , we see a divergence of behaviour between the synthetic data model and the MNIST data, as seen in Figure 5. A plausible cause is violation of the isotropy assumption: correlated features and class structure increase output variance de-

pending on the alignment between \mathbf{v} and high-variance directions.

7 Limitations

Our analysis has several limitations. First, we assume isotropic features and a fixed poisoning (backdoor) direction, which greatly simplifies the random matrix analysis but does not capture more realistic structured covariances or adaptive attack strategies. Second, the clean labels are taken to be randomized and independent of the features, so the model does not include an underlying predictive signal; this allows exact characterization of the poisoning effect but limits direct applicability to typical supervised learning problems where \mathbf{x} carries information about y . Third, we focus on linear ridge regression with an unpenalized intercept, thereby excluding both more complex linear estimators (e.g., with feature-dependent regularization) and the nonlinear models commonly used in practice. Finally, all results are derived in an asymptotic high-dimensional regime, so finite-sample deviations may be non-negligible on real datasets. Extending the framework to structured covariance (e.g., anisotropic features), informative labels, and non-quadratic losses or more general empirical risk minimization problems is an important direction for future work. Extending to anisotropic features would be a feasible extension using an anisotropic deterministic equivalent lemma in place of the Wishart deterministic equivalent. (e.g. Theorem 2.6 from [Couillet & Liao \(2022b\)](#).)

A natural extension of our framework is to models with hierarchical or crossed random effects, which are widely used in large-scale recommendation and feed-ranking systems. In such settings one typically augments a linear or logistic predictor with group-specific random offsets (e.g., user, item, or session effects), estimated via scalable mixed-model machinery (e.g. [Ghosh et al., 2021](#); [Bellio et al., 2025](#)). From a poisoning perspective, this structure creates both challenges and opportunities: an attacker can concentrate corruptions on a specific group or cluster, effectively steering its random effect, and the efficacy of such a targeted attack should depend on the corresponding variance component—large random-effect variances permit substantial group-level deviations from the global trend, while strong shrinkage would attenuate the impact of group-confined poisoning. At the same time, the explicit estimation of random effects and variance components offers potential detection signals, for example by monitoring anomalous group-level effects or abrupt changes in variance estimates over time. Developing an RMT-style analysis of poisoning in these hierarchical models, and formalizing detection criteria based on random-effect diagnostics, is an interesting direction that we leave for future work.

8 Conclusion

We have developed a random matrix framework that quantifies the impact of structured backdoor poisoning in high-dimensional ridge least squares. By deriving closed-form asymptotic laws for the poisoned score, we identified how poisoning rate, trigger strength, regularization, and overparameterization jointly govern attack efficacy. Experiments on synthetic data and MNIST confirm the theory’s predictions, supporting its use as a heuristic lens for more complex models. Looking ahead, extending this analysis to correlated features, nonlinear learners, and modern representation models may provide the same combination of analytic clarity and governance-ready diagnostics that we demonstrated in the linear setting.

9 Acknowledgements

The authors would also acknowledge support from His Majesty’s Government in the development of this research. DF is funded by the Charles Coulson Scholarship.

References

- Article 15: Accuracy, robustness and cybersecurity (eu artificial intelligence act). <https://artificialintelligenceact.eu/article/15/>, a. Accessed 2025-10-01.
- Recital 76 (eu artificial intelligence act): Cybersecurity and data poisoning risks. <https://artificialintelligenceact.eu/recital/76/>, b. Accessed 2025-10-01.
- Mitre atlas: Adversarial threat landscape for artificial-intelligence systems. <https://atlas.mitre.org/>. Accessed 2025-10-01.
- Owasp top 10 for llm applications (archive 2023): Training data poisoning. https://owasp.org/www-project-top-10-for-large-language-model-applications/Archive/0_1_vulns/Training_Data_Poisoning.html, a. Accessed 2025-10-01.
- Owasp genai/llm top 10 (2025): Data and model poisoning. <https://genai.owasp.org/llm-top-10/>, b. Accessed 2025-10-01.
- Matthew Arnold, Rachel K. E. Bellamy, et al. Factsheets: Increasing trust in ai services through supplier’s declarations of conformity. *IBM Journal of Research and Development*, 63(4/5), 2019. doi: 10.1147/JRD.2019.2942288. URL <https://arxiv.org/abs/1808.07261>.
- Zhidong Bai and Jack W. Silverstein. *Spectral Analysis of Large Dimensional Random Matrices*. Springer Series in Statistics. Springer New York, New York, NY, 2010. ISBN 978-1-4419-0660-1 978-1-4419-0661-8. doi: 10.1007/978-1-4419-0661-8. URL <https://link.springer.com/10.1007/978-1-4419-0661-8>. ISSN: 0172-7397.
- Ruggero Bellio, Swarnadip Ghosh, Art B. Owen, and Cristiano Varin. Consistent and Scalable Composite Likelihood Estimation of Probit Models with Crossed Random Effects, April 2025. URL <http://arxiv.org/abs/2308.15681>. arXiv:2308.15681 [stat].
- Miles Brundage, Shahar Avin, Jack Clark, Helen Toner, Peter Eckersley, Ben Garfinkel, Allan Dafoe, Paul Scharre, Thomas Zeitzoff, Bobby Filar, et al. The malicious use of artificial intelligence: Forecasting, prevention, and mitigation. Technical report, Future of Humanity Institute et al., 2018. URL <https://arxiv.org/abs/1802.07228>.
- Nicholas Carlini and Andreas Terzis. Poisoning and Backdooring Contrastive Learning, March 2022. URL <http://arxiv.org/abs/2106.09667>. arXiv:2106.09667 [cs].
- Romain Couillet and Zhenyu Liao. *Random matrix methods for machine learning*. Cambridge University Press, 2022a.
- Romain Couillet and Zhenyu Liao. *Random Matrix Methods for Machine Learning*. Cambridge University Press, 1 edition, July 2022b. ISBN 978-1-009-12849-0 978-1-009-12323-5. doi: 10.1017/9781009128490. URL <https://www.cambridge.org/core/product/identifier/9781009128490/type/book>.
- Li Deng. The MNIST Database of Handwritten Digit Images for Machine Learning Research [Best of the Web]. *IEEE Signal Processing Magazine*, 29(6):141–142, November 2012. ISSN 1558-0792. doi: 10.1109/MSP.2012.2211477. URL <https://ieeexplore.ieee.org/document/6296535>.
- Edinburgh and Stefan Wager. High-dimensional asymptotics of prediction: Ridge regression and classification. *Annals of Statistics*, 46(1):247–279, 2018. doi: 10.1214/17-AOS1554.
- Huaizhi Ge, Yiming Li, Qifan Wang, Yongfeng Zhang, and Ruixiang Tang. When Backdoors Speak: Understanding LLM Backdoor Attacks Through Model-Generated Explanations, November 2024. URL <http://arxiv.org/abs/2411.12701>. arXiv:2411.12701 [cs] version: 1.
- Timnit Gebru, Jamie Morgenstern, Briana Vecchione, Jennifer Wortman Vaughan, Hanna Wallach, Hal Daumé III, and Kate Crawford. Datasheets for datasets. *Communications of the ACM*, 64(12):86–92, 2021. doi: 10.1145/3458723. URL <https://dl.acm.org/doi/10.1145/3458723>.
- Swarnadip Ghosh, Trevor Hastie, and Art B. Owen. Scalable logistic regression with crossed random effects, December 2021. URL <http://arxiv.org/abs/2105.13747>. arXiv:2105.13747 [stat].
- Shafi Goldwasser, Michael P. Kim, Vinod Vaikanathan, and Or Zamir. Planting undetectable backdoors in machine learning models. In *2022 IEEE 63rd Annual Symposium on Foundations of Computer Science (FOCS)*, pp. 931–942. IEEE, 2022.
- Tianyu Gu, Brendan Dolan-Gavitt, and Siddharth Garg. Badnets: Identifying vulnerabilities in the machine learning model supply chain, 2017.
- Trevor Hastie, Andrea Montanari, Saharon Rosset, and Ryan J. Tibshirani. Surprises in high-dimensional ridgeless least squares interpolation. *arXiv preprint arXiv:1903.07571*, 2019.
- Jonathan Hayase, Weihao Kong, Raghav Somani, and Sewoong Oh. SPECTRE: Defending against backdoor attacks using robust statistics. In *Proceedings of the 38th International Conference on Machine Learning Research*, volume 139 of *Proceedings of Machine Learning Research*, pp. 4129–4139. PMLR, 2021.

- Pengfei He, Yue Xing, Han Xu, Zhen Xiang, and Jiliang Tang. Multi-Faceted Studies on Data Poisoning can Advance LLM Development, February 2025. URL <http://arxiv.org/abs/2502.14182>. arXiv:2502.14182 [cs] version: 1.
- Matthew Jagielski, Alina Oprea, Battista Biggio, Chang Liu, Cristina Nita-Rotaru, and Bo Li. Manipulating machine learning: Poisoning attacks and countermeasures for regression learning. In *2018 IEEE Symposium on Security and Privacy (SP)*, pp. 19–35. IEEE, 2018.
- Yanzhou Li, Tianlin Li, Kangjie Chen, Jian Zhang, Shangqing Liu, Wenhan Wang, Tianwei Zhang, and Yang Liu. BadEdit: Backdooring large language models by model editing, March 2024. URL <http://arxiv.org/abs/2403.13355>. arXiv:2403.13355 [cs].
- Naren Sarayu Manoj and Avrim Blum. Excess capacity and backdoor poisoning. In *Advances in Neural Information Processing Systems*, volume 34, pp. 20373–20384, 2021.
- Song Mei, Andrea Montanari, and Phan-Minh Nguyen. Generalization error of random features and kernel methods: Universality, approximate message passing, and kernel ridge regression. *Annals of Statistics*, 47(6):2797–2826, 2019. doi: 10.1214/19-AOS1780.
- Margaret Mitchell, Simone Wu, Andrew Zaldivar, Parker Barnes, Lucy Vasserman, Ben Hutchinson, Elena Spitzer, Inioluwa Deborah Raji, and Timnit Gebru. Model cards for model reporting. In *Proceedings of the ACM Conference on Fairness, Accountability, and Transparency (FAccT)*, 2019. doi: 10.1145/3287560.3287596. URL <https://dl.acm.org/doi/10.1145/3287560.3287596>.
- National Institute of Standards and Technology. Ai risk management framework: Generative ai profile. Technical Report NIST AI 600-1, NIST, 2024. URL <https://nvlpubs.nist.gov/nistpubs/ai/NIST.AI.600-1.pdf>.
- Roy Schwartz, Jesse Dodge, Noah A. Smith, and Oren Etzioni. Green ai. *Communications of the ACM*, 63(12):54–63, 2020. doi: 10.1145/3381831. URL <https://cacm.acm.org/research/green-ai/>.
- Ali Shafahi, W. Ronny Huang, Mahyar Najibi, Octavian Suci, Christoph Studer, Tudor Dumitras, and Tom Goldstein. Poison Frogs! Targeted Clean-Label Poisoning Attacks on Neural Networks. In *Advances in Neural Information Processing Systems*, volume 31. Curran Associates, Inc., 2018. URL https://papers.nips.cc/paper_files/paper/2018/hash/22722a343513ed45f14905eb07621686-Abstract.html.
- Jacob Steinhardt, Pang Wei Koh, and Percy Liang. Certified defenses for data poisoning attacks. In *Advances in Neural Information Processing Systems*, volume 30, 2017.
- Christian Szegedy, Wojciech Zaremba, Ilya Sutskever, Joan Bruna, Dumitru Erhan, Ian Goodfellow, and Rob Fergus. Intriguing properties of neural networks, February 2014. URL <http://arxiv.org/abs/1312.6199>. arXiv:1312.6199 [cs].
- Elham Tabassi et al. Artificial intelligence risk management framework (ai rmf 1.0). Technical Report NIST AI 100-1, National Institute of Standards and Technology, 2023. URL <https://nvlpubs.nist.gov/nistpubs/ai/nist.ai.100-1.pdf>.
- Brandon Tran, Jerry Li, and Aleksander Madry. Spectral signatures in backdoor attacks. In *Advances in Neural Information Processing Systems*, volume 31, pp. 8000–8010, 2018.
- Alexander Turner, Dimitris Tsipras, and Aleksander Madry. Label-Consistent Backdoor Attacks, December 2019. URL <http://arxiv.org/abs/1912.02771>. arXiv:1912.02771 [stat].
- Apostol Vassilev et al. Adversarial machine learning: A taxonomy and terminology of attacks and mitigations. Technical Report NIST AI 100-2 (E2025), National Institute of Standards and Technology, 2025. URL <https://nvlpubs.nist.gov/nistpubs/ai/NIST.AI.100-2e2025.pdf>.
- Roman Vershynin. *High-dimensional probability: an introduction with applications in data science*. Number 47 in Cambridge series in statistical and probabilistic mathematics. University Press, Cambridge, 2018. ISBN 978-1-108-41519-4.
- Martin J. Wainwright. *High-Dimensional Statistics: A Non-Asymptotic Viewpoint*. Cambridge Series in Statistical and Probabilistic Mathematics. Cambridge University Press, Cambridge, 2019. ISBN 978-1-108-49802-9. doi: 10.1017/9781108627771. URL <https://www.cambridge.org/core/books/highdimensional-statistics/8A91ECEEC38F46DAB53E9FF8757C7A4E>.
- Binghui Wang, Xiaoyu Cao, Jinyuan Jia, and Neil Zhenqiang Gong. On certifying robustness against backdoor attacks via randomized smoothing. *arXiv preprint arXiv:2002.11750*, 2020.
- Xun Xian, Xuan Bi, Mingyi Hong, Ganghua Wang, and Jie Ding. Understanding backdoor attacks through the adaptability hypothesis. In *Proceedings of the 40th International Conference on Machine Learning*, volume 202 of *Proceedings of Machine Learning Research*. PMLR, 2023.
- Zhen Xiang, Zidi Xiong, and Bo Li. CBD: A certified backdoor detector based on local dominant probability. In *Advances in Neural Information Processing Systems*, 2023.

- Chulin Xie, Minghao Chen, Pin-Yu Chen, and Bo Li. CRFL: Certifiably robust federated learning against backdoor attacks. In *Proceedings of the 38th International Conference on Machine Learning*, volume 139 of *Proceedings of Machine Learning Research*, pp. 11372–11382. PMLR, 2021.
- Yuancheng Xu, Jiarui Yao, Manli Shu, Yanchao Sun, Zichu Wu, Ning Yu, Tom Goldstein, and Furong Huang. Shadowcast: Stealthy data poisoning attacks against vision-language models. *arXiv preprint arXiv:2402.06659*, 2024.
- Hongwei Yao, Jian Lou, and Zhan Qin. PoisonPrompt: Backdoor Attack on Prompt-based Large Language Models, December 2023. URL <http://arxiv.org/abs/2310.12439>. arXiv:2310.12439 [cs].
- Kaiyuan Zhang, Siyuan Cheng, Guangyu Shen, Guanhong Tao, Shengwei An, Anuran Makur, Shiqing Ma, and Xiangyu Zhang. Exploring the orthogonality and linearity of backdoor attacks. In *2024 IEEE Symposium on Security and Privacy (SP)*. IEEE, 2024a. doi: 10.1109/SP54263.2024.00225.
- Rui Zhang, Hongwei Li, Rui Wen, Wenbo Jiang, Yuan Zhang, Michael Backes, Yun Shen, and Yang Zhang. Instruction Backdoor Attacks Against Customized LLMs, May 2024b. URL <http://arxiv.org/abs/2402.09179>. arXiv:2402.09179 [cs].
- Kangjie Zhou, Pengying Wu, Yao Su, Han Gao, Ji Ma, Hangxin Liu, and Chang Liu. ASPIRE: An Informative Trajectory Planner with Mutual Information Approximation for Target Search and Tracking, March 2024. URL <http://arxiv.org/abs/2403.01674>. arXiv:2403.01674 [cs].
- Xiangyu Zhou, Yao Qiang, Saleh Zare Zade, Mohammad Amin Roshani, Prashant Khanduri, Douglas Zytco, and Dongxiao Zhu. Learning to Poison Large Language Models for Downstream Manipulation, May 2025. URL <http://arxiv.org/abs/2402.13459>. arXiv:2402.13459 [cs] version: 3.

A Appendix

A.1 Proof of Results

In this section we provide full proofs of the results for Theorem 3.1 and Proposition 4.4. The proofs are done using random matrix theory, and particularly the resolvent techniques put forward by [Couillet & Liao \(2022a\)](#).

We use the following notation from [Couillet & Liao \(2022a\)](#):

Definition 1. For $\mathbf{X}, \mathbf{Y} \in \mathbb{R}^{n \times n}$ two random or deterministic matrices, we write

$$\mathbf{X} \longleftrightarrow \mathbf{Y},$$

if, for all $\mathbf{A} \in \mathbb{R}^{n \times n}$ and $\mathbf{a}, \mathbf{b} \in \mathbb{R}^n$ of unit norms (respectively, operator and Euclidean), we have the simultaneous results

$$\frac{1}{n} \operatorname{tr} \mathbf{A}(\mathbf{X} - \mathbf{Y}) \rightarrow 0, \quad \mathbf{a}^\top (\mathbf{X} - \mathbf{Y}) \mathbf{b} \rightarrow 0, \quad \|\mathbb{E}[\mathbf{X} - \mathbf{Y}]\| \rightarrow 0,$$

where, for random quantities, the convergence is either in probability or almost surely.

We then prove the following two deterministic equivalent lemmas, allowing us to understand the spiked resolvent

Lemma A.1. *Suppose \mathbf{X} is a $\mathbb{R}^{p \times n}$ matrix, such that each entry $X_{i,j} \sim N(0, 1)$ is an independent and identically distributed Gaussian random variable. Now $\mathbf{Z} = \mathbf{X} + \tau \sqrt{n} \mathbf{a} \mathbf{b}^\top$, where \mathbf{a} and \mathbf{b} are of unit norm in \mathbb{R}^p and \mathbb{R}^n respectively.*

The spiked resolvent $\mathbf{Q}_1(z) = (\frac{1}{n} \mathbf{Z} \mathbf{Z}^\top - z \mathbf{I}_p)^{-1}$ satisfies the deterministic equivalent

$$\mathbf{Q}_1 \longleftrightarrow \bar{\mathbf{Q}}_1 := m(z) \mathbf{I}_p - m(z) \left(1 - \frac{1}{1 + \tau^2(1 + zm(z))} \right) \mathbf{a} \mathbf{a}^\top$$

Lemma A.2. *Under the same assumptions as above, the square of the spiked resolvent \mathbf{Q}_1^2 satisfies the deterministic equivalent*

$$\mathbf{Q}_1^2 \longleftrightarrow m'(z) \mathbf{I}_p + \left(\frac{m'(z)(\tau^2 + 1) - m(z)^2 \tau^2}{(1 + \tau^2(1 + zm(z)))^2} - m'(z) \right) \mathbf{a} \mathbf{a}^\top$$

In particular, for

$$\tilde{\mathbf{Q}}_1 := \left(\frac{1}{n} \mathbf{Z}^\top \mathbf{Z} - z \mathbf{I}_n \right)^{-1}$$

Then,

$$\tilde{\mathbf{Q}}_1^2 \longleftrightarrow \tilde{m}'(z) \mathbf{I}_n + \left(\frac{(c^{-1} \tau^2 + 1) \tilde{m}'(z) - \tilde{m}(z)^2 \tau^2 c^{-1}}{(1 + c^{-1} \tau^2(1 + z \tilde{m}(z)))^2} - \tilde{m}'(z) \right) \mathbf{b} \mathbf{b}^\top$$

Where $\tilde{m}(z)$ is the Stieltjes transform corresponding to the Gram matrix resolvent $\tilde{\mathbf{Q}}(z)$, and satisfies the relations $\tilde{m}(z) = cm(z) - \frac{1-c}{z}$, and $\tilde{m}'(z) = c^{-1} m_{\text{flip}}'(c^{-1}z)$, where $m_{\text{flip}}(z)$ is the Stieltjes transform obtained by simply substituting c^{-1} for c in the definition of $m(z)$.

A.2 Proof of Proposition 4.4

Proof. We consider first the expectation, we claim that $\mathbb{E}[\hat{\boldsymbol{\beta}}^\top \mathbf{a}] \rightarrow C \mathbf{v}^\top \mathbf{a}$

Then we write,

$$\mathbb{E}[\mathbf{a}^\top \hat{\boldsymbol{\beta}}] = \mathbb{E} \left[\frac{1}{n} \mathbf{a}^\top \mathbf{Q}_1 \tilde{\mathbf{Z}} \tilde{\mathbf{w}} \right] = \sum_{i=1}^n \frac{1}{n} \mathbb{E} [\mathbf{a}^\top \mathbf{Q}_1 \tilde{\mathbf{z}}_i \tilde{w}_i]$$

Then to handle the dependence between \mathbf{Q}_1 and $\tilde{\mathbf{z}}_i$ we employ a trick commonly used in the textbook ([Couillet & Liao, 2022a](#)) of removing the $\tilde{\mathbf{z}}_i$ term from \mathbf{Q}_1 . This amounts to a rank-1 perturbation of $\tilde{\mathbf{Z}} \tilde{\mathbf{Z}}^\top$, which we can then understand the behaviour on \mathbf{Q}_1 through the Sherman–Morrison formula.

Since $\mathbf{Q}_1 = \left(\frac{1}{n} \tilde{\mathbf{Z}} \tilde{\mathbf{Z}}^\top + \lambda \mathbf{I} \right)^{-1} = \left(\frac{1}{n} \sum_{i=1}^n \tilde{\mathbf{z}}_i \tilde{\mathbf{z}}_i^\top + \lambda \mathbf{I} \right)^{-1}$, we define the “leave-one-out” resolvent

$$\mathbf{Q}_1^{-i} = \left(\frac{1}{n} \sum_{j \neq i} \tilde{\mathbf{z}}_j \tilde{\mathbf{z}}_j^\top + \lambda \mathbf{I} \right)^{-1}$$

And using the Sherman–Morrison formula, we compute:

$$\mathbf{Q}_1 \tilde{\mathbf{z}}_i = \frac{\mathbf{Q}_1^{-i} \tilde{\mathbf{z}}_i}{1 + \frac{1}{n} \tilde{\mathbf{z}}_i^\top \mathbf{Q}_1^{-i} \tilde{\mathbf{z}}_i}$$

Then we claim that the denominator here satisfies¹

$$\mathbb{E} \left| \frac{1}{1 + \frac{1}{n} \tilde{\mathbf{z}}_i^\top \mathbf{Q}_1^{-i} \tilde{\mathbf{z}}_i} - \frac{1}{1 + cm(-\lambda)} \right|^2 = \frac{1}{n} \quad (13)$$

To see this we use two facts

1. For $\mathbf{x}_i \sim \mathcal{N}(0, \mathbf{I}_p)$ and \mathbf{A} independent of \mathbf{x}_i with $\|\mathbf{A}\| = O(1)$, then

$$\mathbb{E} \left| \frac{1}{n} \mathbf{x}_i^\top \mathbf{A} \mathbf{x}_i - \text{tr } \mathbf{A} \right|^2 = O(n^{-1}) \quad (14)$$

- 2.

$$\frac{1}{p} \text{tr } \mathbf{Q}_1(-\lambda) = m(-\lambda) + O(n^{-1}) \quad (15)$$

Equation 14 can be seen by an explicit calculation of the variance, or as a special case of Couillet & Liao (2022a) Lemma 2.9. And Equation 15 can be seen by the Sherman Morrison formula, as \mathbf{Q}_1 is a rank 3 perturbation of the Wishart matrix resolvent. Denoting this by $\frac{1}{n} \text{tr } \tilde{\mathbf{Q}}_\lambda = \left(\frac{1}{n} \mathbf{X} \mathbf{X}^\top + \lambda \mathbf{I}_p \right)^{-1}$, it is a standard fact that $\tilde{\mathbf{Q}}_\lambda = m(-\lambda) + O(n^{-1})$, and then by the Woodbury Lemma we see that finite rank perturbations don’t affect the normalised trace.

Following from these facts then, we have that

$$\begin{aligned} \mathbb{E} \left| \frac{1}{1 + \frac{1}{n} \tilde{\mathbf{z}}_i^\top \mathbf{Q}_1^{-i} \tilde{\mathbf{z}}_i} - \frac{1}{1 + cm(-\lambda)} \right|^2 &\leq C \left(\mathbb{E} \left| \frac{1}{n} \tilde{\mathbf{z}}_i^\top \mathbf{Q}_1^{-i} \tilde{\mathbf{z}}_i - \frac{1}{n} \mathbf{x}_i^\top \mathbf{Q}_1^{-i} \mathbf{x}_i \right|^2 + \mathbb{E} \left| \frac{1}{n} \mathbf{x}_i^\top \mathbf{Q}_1^{-i} \mathbf{x}_i - cm(-\lambda) \right|^2 \right) \\ &= O(n^{-1}) \end{aligned}$$

Since as $\tilde{\mathbf{Z}} = \mathbf{X} + \mathbf{v} \mathbf{r}^\top$, then $\tilde{\mathbf{z}}_i = \mathbf{x}_i + \mathbf{v} r_i$, and in particular $\|\tilde{\mathbf{z}}_i - \mathbf{x}_i\| = O(1)$

Returning now to our calculation, we have

$$\mathbb{E}[\mathbf{a}^\top \hat{\boldsymbol{\beta}}] = \sum_{i=1}^n \frac{1}{n} \mathbb{E} \frac{\mathbf{a}^\top \mathbf{Q}_1^{-i} \tilde{\mathbf{z}}_i \tilde{w}_i}{1 + \frac{1}{n} \tilde{\mathbf{z}}_i^\top \mathbf{Q}_1^{-i} \tilde{\mathbf{z}}_i} = \sum_{i=1}^n \frac{1}{n} \mathbb{E} \frac{\mathbf{a}^\top \mathbf{Q}_1^{-i} \tilde{\mathbf{z}}_i \tilde{w}_i}{1 + cm(-\lambda)} + O(n^{-1/2})$$

This comes from using equation 13 along a Hölder inequality and the fact that since $\tilde{\mathbf{z}}_i$ is independent of \mathbf{Q}_1^{-i} , the variance of the numerator is bounded, specifically we have $\mathbb{E} [(\mathbf{a}^\top \mathbf{Q}_1^{-i} \tilde{\mathbf{z}}_i \tilde{w}_i)^2 \mid \mathbf{Q}_1^{-i}] \leq \mathbf{a}^\top (\mathbf{Q}_1^{-i})^2 \mathbf{a} \leq \|\mathbf{a}\|^2 / \lambda^2$ (since $\tilde{w}_i \leq 1$).

Following from these we immediately see on breaking $\tilde{\mathbf{z}}_i = \mathbf{x}_i + \mathbf{v} r_i$ that the \mathbf{x}_i term vanishes, as it is mean 0 and independent. Hence,

¹In fact we can take higher powers here, but the variance is sufficient for our purposes.

$$\begin{aligned}\mathbb{E}[\mathbf{a}^\top \hat{\boldsymbol{\beta}}] &= \frac{1}{1 + cm(-\lambda)} \frac{1}{n} \sum_{i=1}^n \mathbb{E} \mathbf{a}^\top \mathbf{Q}_1^{-i} \mathbf{v} \mathbf{r}_i \tilde{w}_i + O(n^{-1/2}) \\ &= \frac{1}{1 + cm(-\lambda)} \frac{1}{n} \mathbf{a}^\top \bar{\mathbf{Q}}_1 \mathbf{v} \mathbf{r}^\top \tilde{\mathbf{w}} + O(n^{-1/2})\end{aligned}$$

Here we have used Lemma A.1 for the deterministic equivalent of the resolvent.

Finally, we evaluate this limit. From the setup of our problem we see that, $\frac{1}{n} \mathbf{r}^\top \tilde{\mathbf{w}} \xrightarrow{a.s.} \frac{1}{2} \theta (1 - \theta)$ and $\frac{1}{n} \|\mathbf{r}\|^2 \xrightarrow{a.s.} \frac{\theta}{2} (1 - \frac{\theta}{2})$.

Hence, expanding out the deterministic equivalent we get

$$\mathbb{E}[\mathbf{a}^\top \hat{\boldsymbol{\beta}}] = \frac{m(-\lambda) \theta (1 - \theta) \mathbf{a}^\top \mathbf{v}}{(1 + cm(-\lambda)) (2 + \|\mathbf{v}\|^2 \theta (1 - \frac{\theta}{2}) (1 - \lambda m(-\lambda)))}.$$

To show convergence, we then use a concentration of measure argument to say that $\mathbf{a}^\top \hat{\boldsymbol{\beta}} \rightarrow \mathbb{E}[\mathbf{a}^\top \hat{\boldsymbol{\beta}}]$. For this we use the Burkholder inequality for martingale differences.

Lemma A.3 (Burkholder inequality Bai & Silverstein (2010), Lemma 2.13). *Let $\{X_i\}_{i=1}^\infty$ be a martingale difference sequence for the filtration $\{\mathcal{F}_i\}$ and denote by \mathbb{E}_k the conditional expectation with respect to \mathcal{F}_k . Then, for $k \geq 2$, there exists a constant C_k depending only on k such that*

$$\mathbb{E} \left| \sum_{i=1}^n X_i \right|^k \leq C_k \left(\mathbb{E} \left[\sum_{i=1}^n \mathbb{E}_{i-1} (|X_i|^2) \right]^{k/2} + \sum_{i=1}^n \mathbb{E} (|X_i|^k) \right).$$

The utility of this comes by letting the filtration $\mathcal{F}_i = \sigma(\tilde{\mathbf{z}}_1, \dots, \tilde{\mathbf{z}}_i)$, and then writing

$$\mathbf{a}^\top \hat{\boldsymbol{\beta}} - \mathbb{E}[\mathbf{a}^\top \hat{\boldsymbol{\beta}}] = \sum_i (\mathbb{E}_i - \mathbb{E}_{i-1}) (\mathbf{a}^\top \hat{\boldsymbol{\beta}}) = \sum_i (\mathbb{E}_i - \mathbb{E}_{i-1}) (\mathbf{a}^\top \hat{\boldsymbol{\beta}} - \mathbf{a}^\top \hat{\boldsymbol{\beta}}_{-i})$$

Where here we let $\hat{\boldsymbol{\beta}}_{-i}$ be the estimator constructed from missing out data point $(\tilde{\mathbf{z}}_i, \tilde{\mathbf{w}}_i)$. This gives us a concrete way to use the intuition that if we leave out one datapoint it shouldn't change the result, since by the Burkholder inequality, if we can control the moments of $\mathbf{a}^\top \hat{\boldsymbol{\beta}} - \mathbf{a}^\top \hat{\boldsymbol{\beta}}_{-i}$ then can control the fluctuations from the mean. In particular, if we choose $k = 4$ in Burkholder, then we can show that the 4th moment of the left side is $O(n^{-2})$, and hence we have absolute convergence.

Using again Sherman-Morrison, we then get:

$$\mathbf{a}^\top \hat{\boldsymbol{\beta}} - \mathbf{a}^\top \hat{\boldsymbol{\beta}}_{-i} = \mathbf{a}^\top \left(\mathbf{Q}_1^{-i} - \frac{1}{n} \frac{\mathbf{Q}_1^{-i} \tilde{\mathbf{z}}_i \tilde{\mathbf{z}}_i^\top \mathbf{Q}_1^{-i}}{1 + \frac{1}{n} \tilde{\mathbf{z}}_i^\top \mathbf{Q}_1^{-i} \tilde{\mathbf{z}}_i} \right) \left(\frac{1}{n} \sum_{j \neq i} \tilde{\mathbf{z}}_j \tilde{w}_j + \frac{1}{n} \tilde{\mathbf{z}}_i \tilde{w}_i \right) - \mathbf{a}^\top \hat{\boldsymbol{\beta}}_{-i}$$

The first term from each bracket then multiplies to cancel exactly the $\mathbf{a}^\top \hat{\boldsymbol{\beta}}_{-i}$ term. We then need to argue that 4th moments of the remaining terms are small to use Burkholder.

1. $\frac{1}{n} \mathbf{a}^\top \mathbf{Q}_1^{-i} \tilde{\mathbf{z}}_i \tilde{w}_i$. To bound this term, we use independence of $\tilde{\mathbf{z}}_i$ and \mathbf{Q}_1^{-i} to see that it is conditionally normal, with mean and variance depending on $\|\mathbf{Q}_1^{-i} \mathbf{a}\|$. By boundedness of \mathbf{Q}_1^{-i} this term then has for example

$$\mathbb{E} \left[\left| \frac{1}{n} \mathbf{a}^\top \mathbf{Q}_1^{-i} \tilde{\mathbf{z}}_i \tilde{w}_i \right|^4 \right] = O(n^{-4})$$

2. To bound the term

$$\mathbb{E} \left[\left| \frac{1}{n^2} \mathbf{a}^\top \frac{\mathbf{Q}_1^{-i} \tilde{\mathbf{z}}_i \tilde{\mathbf{z}}_i^\top \mathbf{Q}_1^{-i}}{1 + \frac{1}{n} \tilde{\mathbf{z}}_i^\top \mathbf{Q}_1^{-i} \tilde{\mathbf{z}}_i} \tilde{\mathbf{z}}_i \tilde{w}_i \right|^4 \right],$$

we use Hölder's inequality, and positive definiteness of the denominator to get

$$\leq \frac{1}{n^4} \mathbb{E} \left[\left| \mathbf{a}^\top \mathbf{Q}_1^{-i} \tilde{\mathbf{z}}_i \right|^8 \right]^{1/2} \mathbb{E} \left[\left| \frac{1}{n} \tilde{\mathbf{z}}_i^\top \mathbf{Q}_1^{-i} \tilde{\mathbf{z}}_i \right|^8 \right]^{1/2}.$$

The first term is $O(1)$ by the same conditional normal argument as above, while the second term is $O(1)$ by a simple norm bound, and hence we again get the required $O(n^{-4})$.

3. The final term is

$$\begin{aligned} & \mathbb{E} \left[\left| \frac{1}{n^2} \mathbf{a}^\top \frac{\mathbf{Q}_1^{-i} \tilde{\mathbf{z}}_i \tilde{\mathbf{z}}_i^\top \mathbf{Q}_1^{-i}}{1 + \frac{1}{n} \tilde{\mathbf{z}}_i^\top \mathbf{Q}_1^{-i} \tilde{\mathbf{z}}_i} \left(\frac{1}{n} \sum_{j \neq i} \tilde{\mathbf{z}}_j \tilde{w}_j \right) \right|^4 \right] \\ & \leq \frac{1}{n^4} \mathbb{E} \left[\left| \mathbf{a}^\top \mathbf{Q}_1^{-i} \tilde{\mathbf{z}}_i \right|^8 \right]^{1/2} \mathbb{E} \left[\left| \tilde{\mathbf{z}}_i^\top \hat{\boldsymbol{\beta}}_{-i} \right|^8 \right]^{1/2}. \end{aligned}$$

Where we have again used Hölder's inequality and that $\hat{\boldsymbol{\beta}}_{-i} = \frac{1}{n} \mathbf{Q}_1^{-i} \sum_{j \neq i} \tilde{\mathbf{z}}_j \tilde{w}_j$. We can then use a conditional normal argument again, since $\tilde{\mathbf{z}}_i$ is independent from $\hat{\boldsymbol{\beta}}_{-i}$, and note simply that $\|\hat{\boldsymbol{\beta}}_{-i}\|^2$ is absolutely bounded since we may rearrange

$$\|\hat{\boldsymbol{\beta}}\|^2 = \frac{1}{n} \tilde{\mathbf{w}}^\top \left(z \tilde{\mathbf{Q}}_1(z)^2 + \tilde{\mathbf{Q}}_1(z) \right) \tilde{\mathbf{w}}$$

for $\tilde{\mathbf{Q}}_1(z) = \left(\frac{1}{n} \tilde{\mathbf{X}}^\top \tilde{\mathbf{X}} - z \mathbf{I}_n \right)^{-1}$.

Hence, by Burkholder $\mathbb{E}[\|\mathbf{a}^\top \hat{\boldsymbol{\beta}} - \mathbb{E} \mathbf{a}^\top \hat{\boldsymbol{\beta}}\|^4] = O(n^{-2})$, and in particular

$$\mathbf{a}^\top \hat{\boldsymbol{\beta}} \xrightarrow{a.s.} \mathbb{E}[\mathbf{a}^\top \hat{\boldsymbol{\beta}}] = \frac{m(-\lambda)\theta(1-\theta)\mathbf{a}^\top \mathbf{v}}{(1+cm(-\lambda))(2+\|\mathbf{v}\|^2\theta(1-\frac{\theta}{2})(1-\lambda m(-\lambda)))}$$

□

A.3 Proof of Theorem 3.1

Proof. Recall the setup,

$$\tilde{\mathbf{X}} = \mathbf{X} + \mathbf{v} \mathbf{r}^\top, \quad \tilde{\mathbf{w}} = \mathbf{y} + 2\mathbf{r}, \quad \mathbf{r} = \mathbf{u} - \frac{\theta}{2} \mathbf{1},$$

so that

$$\frac{1}{n} \|\mathbf{r}\|^2 \xrightarrow{a.s.} s := \frac{\theta}{2} \left(1 - \frac{\theta}{2} \right), \quad \frac{1}{n} \mathbf{y}^\top \mathbf{r} \xrightarrow{a.s.} -\frac{\theta}{2}.$$

Then by Proposition 4.4 we have that $\hat{\boldsymbol{\beta}}^\top \mathbf{v}$ concentrates to a constant, which we identify as μ . The randomness in $\hat{\boldsymbol{\beta}}^\top (\mathbf{x}_0 + \mathbf{v})$ then comes from \mathbf{x}_0 . Conditionally on $\hat{\boldsymbol{\beta}}$, $\hat{\boldsymbol{\beta}}^\top \mathbf{x}_0 \sim \mathcal{N}(0, \|\hat{\boldsymbol{\beta}}\|^2)$, hence the asymptotic variance is $\sigma^2 = \lim \|\hat{\boldsymbol{\beta}}\|^2$.

Let $z = -\lambda$, $\mathbf{Q}_1(z) = \left(\frac{1}{n} \tilde{\mathbf{X}} \tilde{\mathbf{X}}^\top - z \mathbf{I}_p \right)^{-1}$, $\tilde{\mathbf{Q}}_1(z) = \left(\frac{1}{n} \tilde{\mathbf{X}}^\top \tilde{\mathbf{X}} - z \mathbf{I}_n \right)^{-1}$. Using $\frac{1}{n} \tilde{\mathbf{X}}^\top \mathbf{Q}_1(z)^2 \tilde{\mathbf{X}} = z \tilde{\mathbf{Q}}_1(z)^2 + \tilde{\mathbf{Q}}_1(z)$,

$$\|\hat{\boldsymbol{\beta}}\|^2 = \frac{1}{n} \tilde{\mathbf{w}}^\top \left(z \tilde{\mathbf{Q}}_1(z)^2 + \tilde{\mathbf{Q}}_1(z) \right) \tilde{\mathbf{w}} \Big|_{z=-\lambda}.$$

Set the sample-space spike direction $\bar{\mathbf{b}} = \mathbf{r}/\|\mathbf{r}\|$,

$$\tau^2 := \|\mathbf{v}\|^2 s, \quad a := c^{-1} \tau^2, \quad B(z) := 1 + a(1 + z\tilde{m}(z)), \quad S(z) := \tilde{m}(z) + z\tilde{m}'(z).$$

By Lemmas A.1–A.2,

$$\begin{aligned} \tilde{\mathbf{Q}}_1(z) & \iff \tilde{m}(z) \left(\mathbf{I}_n - \left(1 - \frac{1}{B(z)} \right) \bar{\mathbf{b}} \bar{\mathbf{b}}^\top \right), \\ \tilde{\mathbf{Q}}_1(z)^2 & \iff \tilde{m}'(z) \mathbf{I}_n + \left(T(z) - \tilde{m}'(z) \right) \bar{\mathbf{b}} \bar{\mathbf{b}}^\top, \quad T(z) := \frac{(a+1)\tilde{m}'(z) - a\tilde{m}(z)^2}{B(z)^2}. \end{aligned}$$

A direct algebraic check yields

$$z(T(z) - \tilde{m}'(z)) - \tilde{m}(z) \left(1 - \frac{1}{B(z)}\right) = S(z) \left(\frac{a+1}{B(z)^2} - 1\right).$$

Two scalar Law of Large Numbers (LLN) give

$$\frac{1}{n} \|\tilde{\mathbf{w}}\|^2 \xrightarrow{a.s.} 1 - \theta^2, \quad \frac{1}{n} (\tilde{\mathbf{w}}^\top \bar{\mathbf{b}})^2 = \frac{1}{n} \frac{(\tilde{\mathbf{w}}^\top \mathbf{r})^2}{\|\mathbf{r}\|^2} \xrightarrow{a.s.} \frac{(\mathbb{E}[r_i \tilde{w}_i])^2}{\mathbb{E}[r_i^2]} = \frac{\theta(1-\theta)^2}{2-\theta}.$$

Combining the deterministic equivalents with the LLNs,

$$\frac{1}{n} \tilde{\mathbf{w}}^\top (z \tilde{\mathbf{Q}}_1^2 + \tilde{\mathbf{Q}}_1) \tilde{\mathbf{w}} \implies S(z) \left[\frac{1}{n} \|\tilde{\mathbf{w}}\|^2 + \left(\frac{a+1}{B(z)^2} - 1\right) \frac{1}{n} (\tilde{\mathbf{w}}^\top \bar{\mathbf{b}})^2 \right].$$

Evaluating at $z = -\lambda$ gives the variance

$$\sigma^2 = \left(\tilde{m}(-\lambda) - \lambda \tilde{m}'(-\lambda)\right) \left[(1 - \theta^2) + \left(\frac{1+a}{(1+a(1-\lambda \tilde{m}(-\lambda)))^2} - 1 \right) \frac{\theta(1-\theta)^2}{2-\theta} \right], \quad (16)$$

with $a = c^{-1}\tau^2$ and $\tau^2 = \|\mathbf{v}\|^2 \frac{\theta}{2} (1 - \frac{\theta}{2})$.

Remark A.4 (Unregularized limit). If $\lambda \rightarrow 0$ with $c < 1$, then $S(-\lambda) \rightarrow \frac{c}{1-c}$ and $B(-\lambda) \rightarrow 1 + ac = 1 + \tau^2$. Hence

$$\sigma_0^2 = \frac{c}{1-c} \left[(1 - \theta^2) + \left(\frac{1+c^{-1}\tau^2}{(1+\tau^2)^2} - 1 \right) \frac{\theta(1-\theta)^2}{2-\theta} \right].$$

□

A.4 Proof of Lemma A.1

Proof. The main idea behind the proof is we will establish that $\mathbb{E}\mathbf{Q}_1 = \bar{\mathbf{Q}}_1 + o_{\|\cdot\|}(1)$, where $o_{\|\cdot\|}(1)$ is a matrix with operator norm converging to 0 as $n, p \rightarrow \infty$. We then use a concentration argument to see that $\mathbf{Q}_1 = \bar{\mathbf{Q}}_1 + o_{\|\cdot\|}(1)$, where the difference here converges to 0 in operator norm in probability.

To do this, we will first write \mathbf{Q}_1 in a more convenient form.

We have that $\mathbf{Z} = \mathbf{X} + \tau\sqrt{n}\mathbf{a}\mathbf{b}^\top$, and hence

$$\begin{aligned} \frac{1}{n} \mathbf{Z}\mathbf{Z}^\top &= \frac{1}{n} (\mathbf{X} + \tau\sqrt{n}\mathbf{a}\mathbf{b}^\top) (\mathbf{X} + \tau\sqrt{n}\mathbf{a}\mathbf{b}^\top)^\top \\ &= \frac{1}{n} \mathbf{X}\mathbf{X}^\top + \frac{\tau}{\sqrt{n}} \mathbf{a}\mathbf{b}^\top \mathbf{X}^\top + \frac{\tau}{\sqrt{n}} \mathbf{X}\mathbf{b}\mathbf{a}^\top + \tau^2 \mathbf{a}\mathbf{a}^\top \end{aligned}$$

Then we seek to isolate the low rank component of this by defining block matrices $\mathbf{U}, \mathbf{V} \in \mathbb{R}^{p \times 3}$ such that $\frac{1}{n} \mathbf{Z}\mathbf{Z}^\top = \frac{1}{n} \mathbf{X}\mathbf{X}^\top + \mathbf{U}\mathbf{V}^\top$. We have some freedom in this in how we normalise the entries of \mathbf{U} and \mathbf{V} , so we will choose a normalisation so that each entry of \mathbf{U} and \mathbf{V} has size $O(1)$

So making the choice:

$$\mathbf{U} = \begin{bmatrix} \tau \mathbf{a} & \frac{1}{\sqrt{n}} \mathbf{X}\mathbf{b} & \tau \mathbf{a} \end{bmatrix}$$

$$\mathbf{V} = \begin{bmatrix} \frac{1}{\sqrt{n}} \mathbf{X}\mathbf{b} & \tau \mathbf{a} & \tau \mathbf{a} \end{bmatrix}$$

We now have that $\frac{1}{n} \mathbf{Z}\mathbf{Z}^\top = \frac{1}{n} \mathbf{X}\mathbf{X}^\top + \mathbf{U}\mathbf{V}^\top$

Hence we may use the Woodbury formula to write

$$\mathbf{Q}_1(z) = \mathbf{Q}_0(z) - \mathbf{Q}_0(z)\mathbf{U}(\mathbf{I}_3 + \mathbf{V}^\top \mathbf{Q}_0(z)\mathbf{U})^{-1} \mathbf{V}^\top \mathbf{Q}_0(z)$$

Where \mathbf{I}_3 is the 3×3 identity matrix.

Now defining, $\mathbf{A} = (\mathbf{I}_3 + \mathbf{V}^\top \mathbf{Q}_0(z)\mathbf{U})^{-1}$, then we will argue that we can replace \mathbf{A} with a deterministic matrix $\bar{\mathbf{A}}$. Since $\mathbf{A} \in \mathbb{R}^{3 \times 3}$, we may take limits in each entry of $\mathbf{V}^\top \mathbf{Q}_0 \mathbf{U}$ before inverting to get $\bar{\mathbf{A}}$, and from the finite dimensionality we then have that the operator norm $\|\mathbf{A} - \bar{\mathbf{A}}\| \rightarrow 0$.

Our problem term in the expansion of \mathbf{Q}_1 can then be simplified,

$$\begin{aligned} \mathbb{E} [\mathbf{Q}_0 \mathbf{U} \mathbf{A} \mathbf{V}^\top \mathbf{Q}_0] &= \mathbb{E} [\mathbf{Q}_0 \mathbf{U} \bar{\mathbf{A}} \mathbf{V}^\top \mathbf{Q}_0] + \mathbb{E} [\mathbf{Q}_0 \mathbf{U} (\mathbf{A} - \bar{\mathbf{A}}) \mathbf{V}^\top \mathbf{Q}_0] \\ &= \mathbb{E} [\mathbf{Q}_0 \mathbf{U} \bar{\mathbf{A}} \mathbf{V}^\top \mathbf{Q}_0] + o_{\|\cdot\|}(1) \end{aligned}$$

Since $\|\mathbf{Q}_0\|$, $\|\mathbf{U}\|$, and $\|\mathbf{V}\|$ are all $O(1)$ almost surely. (The operator norm of $\frac{1}{\sqrt{n}}\mathbf{X}$ has finite lim sup).

To actually compute the limit of $\mathbf{V}^\top \mathbf{Q}_0 \mathbf{U}$ we use the following almost sure limit identities where \mathbf{a} and \mathbf{b} represent unit vectors of the appropriate dimension

1.

$$\mathbf{a}^\top \mathbf{Q}_0(z) \mathbf{b} \rightarrow m(z) \mathbf{a}^\top \mathbf{b}$$

This comes directly from the deterministic equivalent of \mathbf{Q}_0

2.

$$\frac{1}{\sqrt{n}} \mathbf{a}^\top \mathbf{Q}_0(z) \mathbf{X} \mathbf{b} \rightarrow 0$$

This comes from the fact that $\mathbb{E} \frac{1}{\sqrt{n}} \mathbf{Q}_0 \mathbf{X} = 0$ and a concentration of measure argument

3.

$$\frac{1}{n} \mathbf{a}^\top \mathbf{X}^\top \mathbf{Q}_0(z) \mathbf{X} \mathbf{b} \rightarrow (zcm(z) + c) \mathbf{a}^\top \mathbf{b}$$

This comes from the identity $\frac{1}{n} \mathbf{X}^\top \mathbf{Q}_0 \mathbf{X} = z(\frac{1}{n} \mathbf{X}^\top \mathbf{X} - z\mathbf{I}_n)^{-1} + \mathbf{I}_n$. For which we can recognise this as (almost) a resolvent of the transposed data matrix \mathbf{X}^\top . This has deterministic equivalent $(z\tilde{m}(z) + 1)\mathbf{I}_n$, where \tilde{m} is the corresponding ‘‘transposed’’ Stieltjes transform. \tilde{m} is a rescaling of m with $c \mapsto c^{-1}$, and then also correcting for the fact that we’re dividing by n instead of p . We may massage out the identity $\tilde{m}(z) = cm(z) - \frac{1-c}{z}$ to give the result

These identities then give

$$\begin{aligned} \mathbf{V}^\top \mathbf{Q}_0 \mathbf{U} &= \begin{pmatrix} \frac{\tau}{\sqrt{n}} \mathbf{b}^\top \mathbf{X}^\top \mathbf{Q}_0 \mathbf{a} & \frac{1}{n} \mathbf{b}^\top \mathbf{X}^\top \mathbf{Q}_0 \mathbf{X} \mathbf{b} & \frac{\tau}{\sqrt{n}} \mathbf{b}^\top \mathbf{X}^\top \mathbf{Q}_0 \mathbf{a} \\ \tau^2 \mathbf{a}^\top \mathbf{Q}_0 \mathbf{a} & \frac{\tau}{\sqrt{n}} \mathbf{a}^\top \mathbf{Q}_0 \mathbf{X} \mathbf{b} & \tau^2 \mathbf{a}^\top \mathbf{Q}_0 \mathbf{a} \\ \tau^2 \mathbf{a}^\top \mathbf{Q}_0 \mathbf{a} & \frac{\tau}{\sqrt{n}} \mathbf{a}^\top \mathbf{Q}_0 \mathbf{X} \mathbf{b} & \tau^2 \mathbf{a}^\top \mathbf{Q}_0 \mathbf{a} \end{pmatrix} \\ &\rightarrow \begin{pmatrix} 0 & zcm(z) + c & 0 \\ \tau^2 m(z) & 0 & \tau^2 m(z) \\ \tau^2 m(z) & 0 & \tau^2 m(z) \end{pmatrix} \end{aligned}$$

and hence,

$$\bar{\mathbf{A}} = \begin{pmatrix} 1 & zcm(z) + c & 0 \\ \tau^2 m(z) & 1 & \tau^2 m(z) \\ \tau^2 m(z) & 0 & 1 + \tau^2 m(z) \end{pmatrix}^{-1}$$

Next we turn to eliminating the randomness in \mathbf{U} and \mathbf{V} . We define the deterministic matrices:

$$\bar{\mathbf{U}} = [\tau \mathbf{a} \quad 0 \quad \tau \mathbf{a}]$$

$$\bar{\mathbf{V}} = [0 \quad \tau \mathbf{a} \quad \tau \mathbf{a}]$$

and claim that

$$\mathbb{E} [\mathbf{Q}_0 \mathbf{U} \bar{\mathbf{A}} \mathbf{V}^\top \mathbf{Q}_0] = \mathbb{E} [\mathbf{Q}_0 \bar{\mathbf{U}} \bar{\mathbf{A}} \bar{\mathbf{V}}^\top \mathbf{Q}_0]$$

To see this, note firstly that $\mathbf{U} - \bar{\mathbf{U}}$ and $\mathbf{V} - \bar{\mathbf{V}}$ only contain terms of the form $\frac{1}{\sqrt{n}} \mathbf{X} \mathbf{b}$. If this term appears on its own in the expansion, then the expectation will be 0 since the matrix will then be an odd function of the centered data matrix \mathbf{X} . It then only remains to show that the cross term $\frac{1}{n} \mathbb{E} [\mathbf{Q}_0 \mathbf{X} \mathbf{b} \mathbf{b}^\top \mathbf{X}^\top \mathbf{Q}_0]$ is of vanishing size.

$$\begin{aligned} \frac{1}{n} \mathbb{E} [\mathbf{Q}_0 \mathbf{X} \mathbf{b} \mathbf{b}^\top \mathbf{X}^\top \mathbf{Q}_0] &= \frac{1}{n} \sum_{i,j=1}^n \mathbb{E} [b_i b_j \mathbf{Q}_0 \mathbf{x}_i \mathbf{x}_j^\top \mathbf{Q}_0] \\ &= \frac{1}{n} \sum_{i=1}^n \mathbb{E} [b_i^2 \mathbf{Q}_0 \mathbf{x}_i \mathbf{x}_i^\top \mathbf{Q}_0] \\ &= \frac{1}{n} \sum_{i=1}^n \mathbb{E} \left[b_i^2 \frac{\mathbf{Q}_0^{-i} \mathbf{x}_i \mathbf{x}_i^\top \mathbf{Q}_0^{-i}}{(1 + \mathbf{x}_i^\top \mathbf{Q}_0^{-i} \mathbf{x}_i)^2} \right] \end{aligned}$$

And then since each term is positive semidefinite, we may conclude:

$$\begin{aligned} \left\| \frac{1}{n} \sum_{i=1}^n \mathbb{E} \left[b_i^2 \frac{\mathbf{Q}_0^{-i} \mathbf{x}_i \mathbf{x}_i^\top \mathbf{Q}_0^{-i}}{(1 + \mathbf{x}_i^\top \mathbf{Q}_0^{-i} \mathbf{x}_i)^2} \right] \right\| &\leq \left\| \frac{1}{n} \sum_{i=1}^n \mathbb{E} [b_i^2 \mathbf{Q}_0^{-i} \mathbf{x}_i \mathbf{x}_i^\top \mathbf{Q}_0^{-i}] \right\| \\ &= \frac{1}{n} \sum_{i=1}^n b_i^2 \|(\mathbf{Q}_0^{-i})^2\| = \|\mathbf{b}\|^2 \|(\mathbf{Q}_0^{-i})^2\| / n = o(1) \end{aligned}$$

Hence finally, we have shown that

$$\mathbb{E} [\mathbf{Q}_0 \mathbf{U} \bar{\mathbf{A}} \mathbf{V}^\top \mathbf{Q}_0] = \mathbb{E} [\mathbf{Q}_0 \bar{\mathbf{U}} \bar{\mathbf{A}} \bar{\mathbf{V}}^\top \mathbf{Q}_0] + o_{\|\cdot\|}(1)$$

where now $\bar{\mathbf{U}} \bar{\mathbf{A}} \bar{\mathbf{V}}^\top$ is a purely deterministic matrix.

We may now argue that we can continue our deterministic replacement and replace the \mathbf{Q}_0 matrices with their deterministic equivalents also. In general it is not true for a deterministic matrix \mathbf{B} that $\mathbf{Q}_0 \mathbf{B} \mathbf{Q}_0 \longleftrightarrow \bar{\mathbf{Q}}_0 \mathbf{B} \bar{\mathbf{Q}}_0$, however in [Couillet & Liao \(2022a\)](#) 2.9.5, it was shown that this does hold true when the matrix \mathbf{B} is of finite rank. Fortunately here, we are in this case since $\bar{\mathbf{U}} \bar{\mathbf{A}} \bar{\mathbf{V}}^\top$ is of rank 3, and so

$$\mathbb{E} [\mathbf{Q}_0 \mathbf{U} \bar{\mathbf{A}} \mathbf{V}^\top \mathbf{Q}_0] = \bar{\mathbf{Q}}_0 \bar{\mathbf{U}} \bar{\mathbf{A}} \bar{\mathbf{V}}^\top \bar{\mathbf{Q}}_0 = o_{\|\cdot\|}(1)$$

To conclude, we first compute

$$\begin{aligned} &\bar{\mathbf{Q}}_0 \bar{\mathbf{U}} \bar{\mathbf{A}} \bar{\mathbf{V}}^\top \bar{\mathbf{Q}}_0 \\ &= m(z) \mathbf{I}_p \begin{bmatrix} \tau \mathbf{a} & 0 & \tau \mathbf{a} \end{bmatrix} \begin{pmatrix} 1 & zcm(z) + c & 0 \\ \tau^2 m(z) & 1 & \tau^2 m(z) \\ \tau^2 m(z) & 0 & 1 + \tau^2 m(z) \end{pmatrix}^{-1} \begin{bmatrix} 0 \\ \tau \mathbf{a}^\top \\ \tau \mathbf{a}^\top \end{bmatrix} m(z) \mathbf{I}_p \end{aligned}$$

And after the algebra, and using the identity $zcm(z)^2 - (1 - c - z)m(z) + 1 = 0$, we arrive at the result

$$\bar{\mathbf{Q}}_0 \bar{\mathbf{U}} \bar{\mathbf{A}} \bar{\mathbf{V}}^\top \bar{\mathbf{Q}}_0 = m(z) \left(1 - \frac{1}{1 + \tau^2(1 + zm(z))} \right) \mathbf{a} \mathbf{a}^\top$$

And therefore

$$\begin{aligned} \mathbb{E}[\mathbf{Q}_1] &= \bar{\mathbf{Q}}_0 + \bar{\mathbf{Q}}_0 \bar{\mathbf{U}} \bar{\mathbf{A}} \bar{\mathbf{V}}^\top \bar{\mathbf{Q}}_0 + o_{\|\cdot\|}(1) \\ &= m(z) \left(\mathbf{I}_p - \mathbf{a} \mathbf{a}^\top \left(1 - \frac{1}{1 + \tau^2(1 + zm(z))} \right) \right) + o_{\|\cdot\|}(1) \end{aligned}$$

Remark A.5 (On concentration of measure). Now that we have established the expectation, showing concentration of measure can be done by standard arguments. We don't write this out in full here, as they are very similar to the arguments already done for the concentration of $\mathbf{a}^\top \hat{\beta}$ in the proof of Proposition 4.4. To control the concentration of $\text{tr} \mathbf{A} \mathbf{Q}_1$ and $\mathbf{a}^\top \mathbf{Q}_1 \mathbf{b}$, a martingale Burkholder argument can similarly be applied, allowing us to derive almost sure convergence of these functionals to their mean, by controlling the difference $\mathbf{Q}_1 - \mathbf{Q}_1^{-i}$.

□

A.5 Proof of Lemma A.2

Proof. We aim to compute a deterministic equivalent for \mathbf{Q}_1^2 . There are tempting but wrong routes. First, one might claim $\mathbf{Q}_1^2 \longleftrightarrow (\bar{\mathbf{Q}}_1)^2$, which is false since $\mathbb{E}[\mathbf{Q}_1^2] \neq (\mathbb{E}[\mathbf{Q}_1])^2$.

Next, since $\mathbf{Q}_1(z) = (\frac{1}{n} \mathbf{Z} \mathbf{Z}^\top - z \mathbf{I})^{-1}$, we have $\frac{d}{dz} \mathbf{Q}_1 = \mathbf{Q}_1^2$, so one could guess $\mathbf{Q}_1^2 \longleftrightarrow \frac{d}{dz} \bar{\mathbf{Q}}_1$. This is also wrong because $\mathbb{E}[\mathbf{Q}_1] = \bar{\mathbf{Q}}_1 + o_{\|\cdot\|}(1)$ does not ensure the remainder stays small after differentiation. For the unpoisoned resolvent \mathbf{Q}_0 , (Couillet & Liao, 2022a, 2.9.5) gives $\mathbf{Q}_0^2 \longleftrightarrow m'(z) \mathbf{I}_p$.

We use $\mathbf{A}^{-1} - \mathbf{B}^{-1} = \mathbf{A}^{-1}(\mathbf{B} - \mathbf{A})\mathbf{B}^{-1}$, which converts differences of resolvents into differences of their inverses.

We also use

$$\mathbf{Q}_1 \longleftrightarrow \bar{\mathbf{Q}}_1 = m(z) \left(\mathbf{I}_p - \mathbf{a} \mathbf{a}^\top \left(1 - \frac{1}{1 + \tau^2(1 + zm(z))} \right) \right),$$

so by Sherman–Morrison,

$$\bar{\mathbf{Q}}_1^{-1} = \frac{1}{m(z)} [\mathbf{I}_p + \tau^2(1 + zm(z)) \mathbf{a} \mathbf{a}^\top].$$

Using $m(z) = (\frac{1}{1 + cm(z)} - z)^{-1}$, this is

$$\bar{\mathbf{Q}}_1^{-1} = \left(\frac{1}{1 + cm(z)} - z \right) \mathbf{I}_p + \frac{\tau^2}{1 + cm(z)} \mathbf{a} \mathbf{a}^\top.$$

Now,

$$\begin{aligned} \mathbb{E}[\mathbf{Q}_1^2] &= \mathbb{E}[\mathbf{Q}_1 \bar{\mathbf{Q}}_1] + \mathbb{E}[\mathbf{Q}_1(\mathbf{Q}_1 - \bar{\mathbf{Q}}_1)] = \bar{\mathbf{Q}}_1^2 + \mathbb{E}[\mathbf{Q}_1^2((\bar{\mathbf{Q}}_1)^{-1} - \mathbf{Q}_1^{-1})] \bar{\mathbf{Q}}_1 \\ &= \bar{\mathbf{Q}}_1^2 + \mathbb{E} \left[\mathbf{Q}_1^2 \left(\frac{1}{1 + cm(z)} \mathbf{I}_p - \frac{1}{n} \mathbf{Z} \mathbf{Z}^\top + \frac{\tau^2}{1 + cm(z)} \mathbf{a} \mathbf{a}^\top \right) \right] \bar{\mathbf{Q}}_1 \\ &= \bar{\mathbf{Q}}_1^2 + \frac{\mathbb{E}[\mathbf{Q}_1^2] \bar{\mathbf{Q}}_1}{1 + cm(z)} - \frac{1}{n} \sum_{i=1}^n \mathbb{E}[\mathbf{Q}_1^2 \mathbf{z}_i \mathbf{z}_i^\top] \bar{\mathbf{Q}}_1 + \frac{\tau^2}{1 + cm(z)} \mathbb{E}[\mathbf{Q}_1^2] \mathbf{a} \mathbf{a}^\top \bar{\mathbf{Q}}_1. \end{aligned}$$

For the middle term, use Sherman–Morrison to isolate the contribution of \mathbf{z}_i in \mathbf{Q}_1 and then add and subtract $\bar{\mathbf{Q}}_1$:

$$\begin{aligned} \frac{1}{n} \sum_{i=1}^n \mathbb{E}[\mathbf{Q}_1^2 \mathbf{z}_i \mathbf{z}_i^\top] \bar{\mathbf{Q}}_1 &= \frac{1}{n} \sum_{i=1}^n \mathbb{E} \left[\frac{\mathbf{Q}_1 \mathbf{Q}_1^{-i} \mathbf{z}_i \mathbf{z}_i^\top \bar{\mathbf{Q}}_1}{1 + \frac{1}{n} \mathbf{z}_i^\top \mathbf{Q}_1^{-i} \mathbf{z}_i} \right] \\ &= \frac{1}{n} \sum_{i=1}^n \mathbb{E} \left[\frac{(\mathbf{Q}_1^{-i})^2 \mathbf{z}_i \mathbf{z}_i^\top \bar{\mathbf{Q}}_1}{1 + \frac{1}{n} \mathbf{z}_i^\top \mathbf{Q}_1^{-i} \mathbf{z}_i} \right] - \frac{1}{n} \sum_{i=1}^n \mathbb{E} \left[\frac{\frac{1}{n} \mathbf{Q}_1^{-i} \mathbf{z}_i \mathbf{z}_i^\top (\mathbf{Q}_1^{-i})^2 \mathbf{z}_i \mathbf{z}_i^\top \bar{\mathbf{Q}}_1}{(1 + \frac{1}{n} \mathbf{z}_i^\top \mathbf{Q}_1^{-i} \mathbf{z}_i)^2} \right]. \end{aligned}$$

Using the Quadratic Form Close-to-Trace lemma,

$$\frac{1}{n} \sum_{i=1}^n \mathbb{E}[\mathbf{Q}_1^2 \mathbf{z}_i \mathbf{z}_i^\top] \bar{\mathbf{Q}}_1 = \frac{1}{n} \sum_{i=1}^n \mathbb{E} \left[\frac{(\mathbf{Q}_1^{-i})^2 \mathbf{z}_i \mathbf{z}_i^\top \bar{\mathbf{Q}}_1}{1 + cm(z)} \right] - \frac{1}{n} \sum_{i=1}^n \mathbb{E} \left[\left(\frac{1}{n} \text{tr}(\mathbf{Q}_1^{-i})^2 \right) \frac{\mathbf{Q}_1^{-i} \mathbf{z}_i \mathbf{z}_i^\top \bar{\mathbf{Q}}_1}{(1 + cm(z))^2} \right] + o_{\|\cdot\|}(1).$$

Since $\mathbb{E}[(\mathbf{Q}_1^{-i})^2] = \mathbb{E}[\mathbf{Q}_1^2] + o_{\|\cdot\|}(1)$ and $\mathbb{E}[\frac{1}{n} \sum_{i=1}^n \mathbf{z}_i \mathbf{z}_i^\top] = \mathbf{I}_p + \tau^2 \mathbf{a} \mathbf{a}^\top$, and finite-rank perturbations do not affect normalized traces,

$$\frac{1}{n} \text{tr}(\mathbf{Q}_1^{-i})^2 = \frac{1}{n} \text{tr} \mathbf{Q}_0^2 + o(1) = cm'(z) + o(1).$$

Therefore

$$\begin{aligned}
 \mathbb{E}[\mathbf{Q}_1^2] &= \bar{\mathbf{Q}}_1^2 + \frac{1}{n} \sum_{i=1}^n \mathbb{E} \left[\frac{cm'(z)}{(1+cm(z))^2} \mathbf{Q}_1^{-i} \mathbf{z}_i \mathbf{z}_i^\top \bar{\mathbf{Q}}_1 \right] + o_{\|\cdot\|}(1) \\
 &= \bar{\mathbf{Q}}_1^2 \left[\left(1 + \frac{cm'(z)}{(1+cm(z))^2} \right) \mathbf{I}_p + \frac{\tau^2 cm'(z)}{(1+cm(z))^2} \mathbf{a} \mathbf{a}^\top \right] \\
 &= \frac{1}{m^2(z)} \bar{\mathbf{Q}}_1^2 \left[m'(z) \mathbf{I}_p + \tau^2 (m'(z) - m^2(z)) \mathbf{a} \mathbf{a}^\top \right] \\
 &= m'(z) \mathbf{I}_p + \left(\frac{m'(z)(\tau^2 + 1) - m(z)^2 \tau^2}{(1 + \tau^2(1 + zm(z)))^2} - m'(z) \right) \mathbf{a} \mathbf{a}^\top.
 \end{aligned}$$

□